Send Orders for Reprints to reprints@benthamscience.ae

The Open Construction and Building Technology Journal, **2014,** *8,* **(Suppl 1: M5) 227-247**

Open Access

Experimental Analysis on the Cyclic Response of Beam to Column Joints: State-of-the-Art at Salerno University

M. Latour* and G. Rizzano

University of Salerno - Department of Civil Engineering, Salerno, Italy

Abstract: Aiming to provide a contribution to the codification of design rules for dissipative joints to be applied to MRFs, in last five years, a comprehensive experimental and analytical work dealing with the cyclic behaviour of beam-to-column joints has been developed by the research group of the University of Salerno. In particular, the activity has regarded the study of both classical and innovative typologies characterized by the same initial stiffness and resistance but by different hysteretic behaviours due to the different source of energy dissipation supply imposed in the design process. In this paper, the main results of such a study, performed at the laboratory of materials and structures of the University of Salerno, are reported in order to provide an overview on the main mechanisms involved in the energy dissipation of partial-strength connections. A particular attention is given to the design issues by presenting the procedures aimed at providing to the joints adequate characteristics in terms of stiffness, resistance and ductility supply by hierarchically controlling the behaviour of the single joint components. Furthermore, the results of tested joints (classical and innovative) are compared in terms of hysteretic behaviour and energy dissipation supply in order to point out the advantages of the different connecting systems.

Keywords: Connections, Cyclic, Design, Experimental, MRFs.

1. INTRODUCTION

According to performance based design, in seismic prone areas, the dissipation of the earthquake input energy has to be provided by the yielding of some selected zones, namely dissipative zones, which have to be properly detailed in order to be adequately ductile under cyclic loads [1].

Following the most recent codes, Moment Resisting Frames (MRFs) can be designed according to two opposite strategies. The first one provides to dissipate the seismic input energy in beams, the second one provides to concentrate the plasticization in connections. In the former case, joints are designed to be full-strength in order to allow, under severe seismic events, the full development of the plastic hinges at beam ends [2, 3]. Conversely, in the latter case, connections are designed to be partial strength with respect to the connected beam, so that the seismic input energy is dissipated through the yielding of the joint components. This last approach, as already demonstrated by [4] is particularly cost/effective in case of low-rise frames characterized by long spans, where the design of beams is governed by dead loads and, by adopting partial strength joints, only a part of the bending moment is transferred to the columns. In addition, economic advantages deriving by the adoption of partial strength beam-to-column joints within MR-frames have been already pointed out also for braced frames where the use of partial strength connections can lead to important savings in the gravity load system.

*Address correspondence to this author at the University of Salerno - Department of Civil Engineering, Salerno, Italy;
Tel: +39089 964342; Fax: +39089 964342;
E-mail: mlatour@unisa.it

The strong interest of the scientific community to solutions adopting partial strength joints is reflected also in last version of EC3 and EC8 [5-7]. In fact, the codes, after several decades of researches focused on the study of the mechanisms of energy dissipation of joints, have finally opened the door to the adoption of partial strength joints, explicitly defining the rules to be respected in order to apply such solutions in practical cases.

Even though a significant work has already been carried out by the scientific community [8-14] and, even though a great effort has been devoted by the European Commission towards the codification of the main rules for the application of partial strength joints in semi-continuous frames, the use of such solutions is still far from the common practice. In fact, the code requires that in the design phase, the dissipative capacities of the joints have to be certified and demonstrated by means of experimental testing. As far as it is clear that such requirement is out from the possibilities of common designers, it means that, in order to provide specific rules for the design of dissipative joints to be used in seismic zones, new experimental and theoretical efforts are still needed towards the individuation of a procedure for the prequalification of joints similar to that provided by the AISC code [15].

To this scope, aiming to perform a further step towards the codification of design rules for dissipative joints, in last five years a significant experimental and analytical activity has been devoted to this topic by the research group of the University of Salerno [16-21]. In particular, to date, the experimental activity performed has regarded classical and innovative joint solutions which, according to the basic principle proposed by the research group of dissipating the seis-

1874-8368/14

mic energy always in a specific joint component (i.e. the weakest joint component), can be divided as follows:

Classical Solutions

- Extendend end-plate joints, dissipating in the shear panel;
- Extendend end-plate joints, dissipating in the end-plate;
- Extendend end-plate joints, dissipating at the beam end by applying the Reduced Beam Section technique;
- Double split tee joints, dissipating in the T-stubs flange plates;

Innovative Solutions

- Double split tee joints with hourglass T-stubs, dissipating in X-shaped dampers realized reducing the section of the T-stub flange plate;
- Double split tee joints equipped with friction dampers, dissipating in friction dampers located in between the T-stub web and beam flange;

The study summarized in this paper has been developed by applying a systematic procedure for the design and testing of each joint. In particular, for each analysed joint, the rules to model the components have been defined. Afterwards, a set of rules has been developed and applied to design the specimens which have been successively tested in order to verify the accuracy of the applied procedure. In the following, the main results of the activities performed at the laboratory of materials and structures of the University of Salerno are reported and commented in order to provide an overview to the main mechanisms involved in the energy dissipation of partial-strength connections. A particular attention is provided to the design issues. To this scope procedures aimed at providing to the tested joints adequate characteristics in terms of resistance and ductility supply are presented and verified against the experimental results.

2. DISSIPATION CAPACITY OF THE JOINT COMPONENTS

As already underlined by many past experimental activities, connections can dissipate a significant amount of energy, but their behaviour can be very variable in terms of ductility, energy dissipation and shape of the hysteresis cycles, depending on the joint components involved in the plastic mechanism. In general, depending on the connection, it is possible to individuate three typologies of hysteretic loops:

- a first typology of hysteretic loops is characterized by a stable behaviour with almost constant energy dissipation even at large amplitude cycles (Fig. **1a**);
- a second typology is characterized by stable behaviour in terms of resistance, but a marked stiffness degradation (Fig. **1b**);
- a third typology, characterized by strength and stiffness degradation resulting in pinching phenomena. In this case, the energy dissipation significantly decreases as far as the number of cycles (Fig. **1c**).

In order to govern the dissipative capacities of joints, first of all, a basic distinction has to be made between dissipative and non-dissipative components, in order to make a distinction in the design phase between dissipative and non-dissipative failure mechanisms [2, 22, 23].

Qualitatively, making reference to the joint components defined in the method reported in last version of EC3, basing on the past experiences, it is possible to individuate the dissipative characteristics of each component and some basic principles to be followed in the design of connections to be applied to semi-continuous frames (Table **1**).

First of all, it is well known that local buckling phenomena can limit the development of dissipative mechanisms and therefore, in case of beam-to-column joints, failure modes relying on the plasticization of plates in compression and, more specifically, of the ***column web in compression*** have to be avoided. It is for this reason that, normally, the use of ribs, such as continuity plates, should be commonly suggested in order to obtain satisfactory performances under cyclic loads. Regarding the ***bolts***, it is important to underline that, both under normal and shear stresses, their limited plastic deformation capacity and fatigue life can lead to a brittle collapse of the joint, so that, generally, it is advisable to design them with a sufficient over strength. In particular, they have to be over strengthened also because, their plastic engagement can affect also the behaviour of joint components that normally could provide significant energy dissipation supply, such as ***end-plate, column flange*** and ***flange cleats***

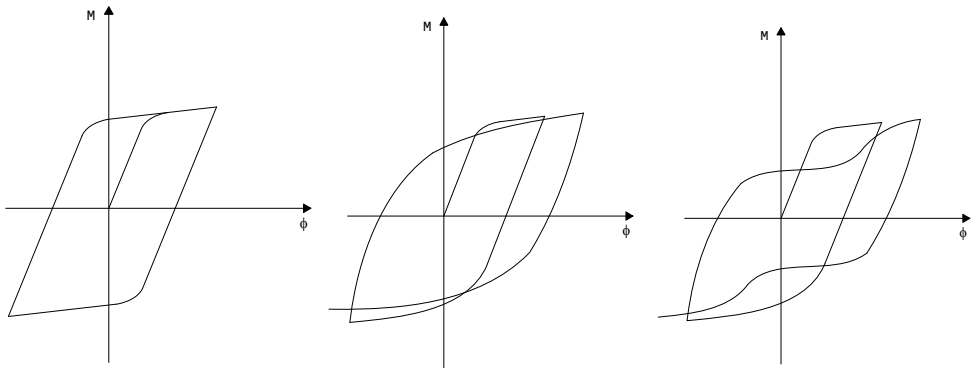

a) Stable Behavior b) Stable with stiffness degradation c) Unstable behavior with pinching

Fig. (1). Moment-rotation response of Joints.

Table 1. Dissipation capacity of the single joint components.

Component		Dissipative	Non Dissipative
Web panel in shear		**X**	
Column web in compression	*Crushing resistance*	**X**	
	Buckling resistance		**x**
Column web in tension		**X**	
Column flange in bending	*Welded joints*		**x**
	Bolted joints	**X**	
End-plate in bending		**X**	
Beam web in tension		**X**	
Plate in tension		**X**	
Plate in compression	*Crushing resistance*	**X**	
	Buckling resistance		**x**
Bolts in tension			**x**
Bolts in shear			**x**

in bending. In fact, the occurrence of plastic deformations in the bolts shanks can result in slips leading to the so-called pinching phenomena.

Similarly, aiming to assure a dissipative behaviour, failure of ***welds*** has to be absolutely avoided, because of their marked brittle behaviour. It is for this reason that, it is normally suggested to provide sufficient over-strength with respect to actions corresponding to the design flexural resistance of the joint also to the welds. Finally, also the yielding of the ***panel zone in shear*** can lead to a significantly dissipative behaviour but, in practical applications, its contribution has to be limited in order to reduce the lateral displacements of the frame and also because high panel deformations can lead to the premature fracture of welds due to stresses concentrations. In fact, to this scope, Eurocode 8 [7], requires that column web panel in shear do not have to contribute for more than the 30% to the plastic rotation capacity of the joint.

3. EXPERIMENTAL ANALYSIS ON BEAM TO COLUMN CONNECTIONS

As aforesaid, in order to investigate the behaviour of connections, in a work conducted since 2011 at the University of Salerno, the behaviour of several connection typologies has been investigated from the dissipative point of view. In particular, to date, eleven full scale tests on beam-to-column connections have been carried out employing always the same beam-column coupling in order to compare easily the results in terms of energy dissipation capacity.

The experimental programme has been developed at the laboratory on materials and structures of the University of Salerno. Two steel hinges, designed to resist shear actions up to 2000 kN and bolted to the carriage base have been employed to connect the specimens to the reacting system. The specimens are assembled with the column (HEB 200) in horizontal position, connected to the hinges, and the beam (IPE 270) in vertical position (Fig. **2**). The loads have been applied by means of two different hydraulic actuators. The first one is a MTS 243.60 actuator with a load capacity equal to 1000 kN in compression and 650 kN in tension with a piston stroke equal to +/- 125 mm which has been used to apply, under force control, the axial load in the column equal to the 30% of the squash load. The second actuator is a MTS 243.35 with load capacity equal to 250 kN both in tension and in compression and a piston stroke equal to +/- 500 mm which has been used to apply, under displacement control, the desired displacement history at the beam end. In order to avoid the lateral-torsional buckling of the beam an horizontal frame has been employed. The geometry of the frame is defined in order to work as a guide which restrains the lateral displacement of the beam and allows the beam rotations. The loading history has been defined in terms of drift angle, according to the protocol provided by [15].

During the tests many parameters have been monitored and acquired, in order to get the test machine history imposed by the top actuator and the displacements of the different joint components. Aiming at the evaluation of the beam end displacements due to the beam-to-column joint rotation only, the displacements measured by means of the LVDT equipping MTS 243.35 have been corrected by subtracting the elastic contribution due to the beam and column flexural deformability according to the following relationship:

$$\delta_j = \delta_{T3} - \frac{FL_b^3}{3EI_b} - \frac{FL_cL_b^2}{12EI_c}\left[\left(\frac{L_c}{L_c+2a}\right)^2 + \frac{6a}{L_c+2a}\right] \qquad (1)$$

where I_b and I_c are the beam and column inertia moments, L_c is the column length, L_b is the beam length and a is the length of the rigid parts, due to the steel hinges (Fig. **3**).

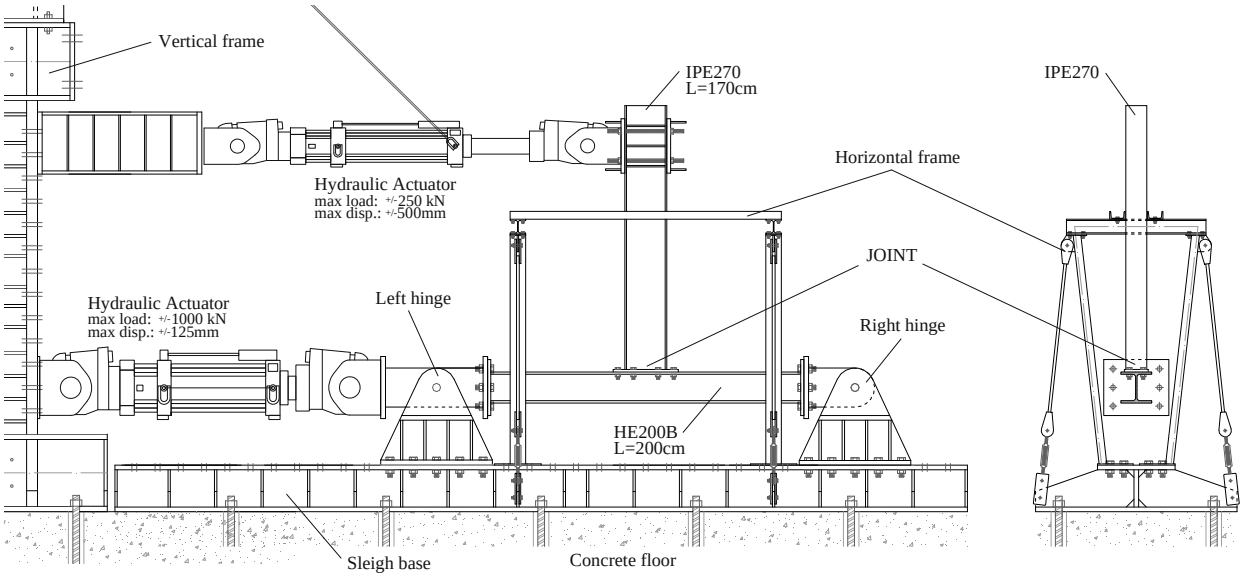

Fig. (2). Experimental setup for tests on joints.

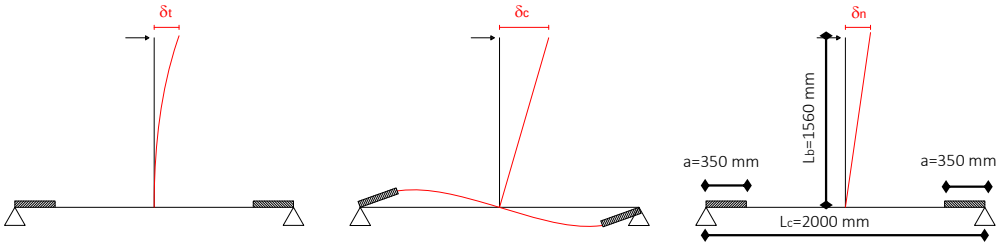

Fig. (3). Scheme for evaluating the joint contribution to the overall rotation.

The experimental program carried out has concerned the following specimens:

- ***EEP-CYC 01*** is a partial strength extended end-plate joint having the panel zone as weakest joint component;
- ***EEP-CYC 02*** is a partial strength extended end-plate joint having the end-plate in bending as weakest joint component;
- ***EEP-DB-CYC 03*** is a full strength extended end-plate joint designed forcing the development of plastic hinge in the beam by cutting the beam flanges following the design criteria for the reduced beam section (RBS) strategy;
- ***TS-CYC 04 – TS-CYC 05*** are partial strength joints with a couple of T-stubs bolted to the beam flanges and to the column flanges, designed to be the main source of plastic deformation capacity;
- ***TSJ-XSCYC 06/ TSJ-XSCYC 07***, which are two partial strength joints with a couple of bolted X-shaped T-stubs, designed to be the main source of plastic deformation. In first case M20 bolts have been adopted to fasten the T-stub flange to the column. In second case M30 bolts have been employed;
- ***TSJ-M1CYC08, TSJ-M2CYC09, TSJ-M2-DSCYC10 and TSJ-BCYC11,*** are double split tee connections with couple of friction dampers realized slotting the tee webs and interposing in between the T-stubs and the beam flanges layers of friction material. The first three joint with layers of friction material called M1 and M2 [24], and the fourth one with a brass plate. The slipping interfaces have been clamped by means of eight M20 class 10.9 bolts tightened with a torque equal to 460 Nm. Joint TSJ-M2-DS-10 has the particularity to employ annular disc springs which are interposed between the bolt nut and the beam flange;

The identity tag individuates uniquely the test. In particular, the meaning of the letters is: 1- Joint typology, i.e. Tee Stub Joint (TSJ), Extended End Plate (EEP), Dog-Bone (EEP-DB), Tee Stub Joint with Haunch (TSJ-H) / 2 – Friction interface, i.e. Friction material M1 (M1), Friction material M2, Brass (B), Sprayed Aluminium (SA) / 3 – Type of washer employed in the test (DS stands for Disc Spring, otherwise is a normal flat washer) / 4 – Progressive number of cyclic tests, i.e. CYCXX.

In the following the applied design procedures and the main results of the experimental activity are here reported.

3.1. Design of the Specimens

In the following the procedures applied to design the specimens of the experimental programme are reported. As aforesaid, the dissipative capacities of beam-to-column joints are mainly governed by the cyclic behaviour of the weakest joint component. Therefore, in all the procedure successively reported, a design based on the application of a hierarchy criterion at the level of the joint components is applied in order to govern the energy dissipation of the joint. The reported procedures can be effectively applied to design connections to be used in different structural typologies applying procedures specifically devoted to the failure mode control and to the localization of the dissipative zones in the connections [25-29].

Design of Specimen EEP-CYC 01

The first joint designed within the experimental programme is a partial strength connection whose resistance is calibrated in order to concentrate the energy dissipation in the shear panel. In order to obtain such a goal, the joint is designed so that the panel zone in shear is the weakest joint component, while the other components are properly over-strengthened.

Design of the Weakest Joint Component

The dissipative component of the joint, i.e. the ***shear panel***, is modelled by means of [30] model. According to this approach, the yield strength of the panel zone is given by the product of three terms:

$$M_y = K_e C_y \gamma_y \tag{2}$$

where, the elastic stiffness is calculated considering both the shear stiffness of the column web panel and the contribution due to the flexural stiffness of the column flanges (K_e), an average shear deformation factor accounting for the distribution of shear stresses in the panel zone at yielding (C_y) and the shear deformation (γ_y).In the elastic range, the shear deformation of the panel zone is computed as the sum of the contribution due to the column web panel and the contribution due to the column flanges:

$$\delta = \left(\frac{1}{k_b} + \frac{1}{k_s} \right) V_{pz} \tag{3}$$

where, with reference to the tested specimen:

$$k_b = \frac{C_r E I_c}{\left[\left(d_b - t_{bf} \right) / 2 \right]^3} = \frac{5 \cdot 210000 \cdot 56960000}{\left[(270 - 10) / 2 \right]^3} = 27222576 \, N/mm \tag{4}$$

$$k_s = \frac{G(A_{vc} + R_f A_{dp})}{\left[\left(d_b - t_{bf} \right) / 2 \right]} = \frac{80769 \cdot 2483}{\left[(270 - 10) / 2 \right]} = 1542688 \, N/mm \tag{5}$$

Where C_r assumed as equal to *5* as suggested by [30], E and G are the elastic and the shear modulus, respectively, I_c is the moment of inertia of the column section, d_c is the column depth, A_{vc} is the column web shear area, A_{dp} is the shear area of doubler plates if adopted in the structural detail and R_f is a factor accounting for the strain incompatibility between supplementary web plates and column web panel. Therefore, the joint rotational stiffness due to the panel zone in shear is given by:

$$K_e = \frac{k_b k_s}{k_b + k_s} \frac{\left(d_b - t_{bf} \right)}{2} \frac{\left(d_b - t_{bf} \right)}{\beta} = \\ = \frac{27222576 \cdot 1542688}{27222576 + 1542688} \frac{(270 - 10)^2}{2 \cdot 1} = 4.93 \cdot 10^{10} \; Nmm/rad \tag{6}$$

The product $C_y \gamma_y$ in Eq.(2) is assumed equal to 0.85 according to the suggestion of [30]. The shear deformation has to be computed accounting also for the interaction between shear stress and normal stress due to the column axial force. Therefore, taking into account that for the tested specimens a constant axial force equal to 30% of the squash load has been applied, according to Von Mises yield criterion, the shear deformation at yielding is given by:

$$\gamma_y = \frac{f_y}{\sqrt{3} G} \sqrt{1 - \left(\frac{P}{P_y} \right)^2} = \frac{355}{\sqrt{3} \cdot 80769} \sqrt{1 - (0.3)^2} = 0.00242 \tag{7}$$

Finally, the bending moment corresponding to the yielding of panel zone in shear is computed by means of Eq.(2):

$$M_{y,pz} = 4.93 \cdot 10^{10} \cdot 0.85 \cdot 0.00242 = 1.01 \cdot 10^8 \, Nmm = 101 \; kNm \tag{8}$$

Considering that the plastic moment of the connected beam (IPE270) is given by:

$$M_{pb} = W_{pl} f_y = 484000 \cdot 275 = 1.33 \cdot 10^8 \, Nmm = 133 \; kNm \tag{9}$$

Derives the following classification in terms of strength:

$$\eta_{ps} = \frac{M_{y,pz}}{M_{pb}} = \frac{101}{133} = 0.759 \tag{10}$$

Therefore, according to the established hierarchy at the level of the joint components, as far as the resistance of the shear panel is defined, the design of the end-plate and of the panels in tension/compression can be carried out providing them a proper over strength.

Design of Non-Dissipative Components

The ***end-plate*** in bending, following the simplified approach provided by Eurocode 3, can be modelled by means of an equivalent T-stub in tension, composed by only the first two bolt rows which are assumed disconnected from the beam web. In particular, assuming that the geometrical parameters of the T-stub are: $m = d - 0.8\sqrt{2}a = 45 - 0.8 \cdot 10 = 37mm$, $n = 45mm$ and $b = 154mm$, it is possible to design the end-plate thickness. The loadings acting on the T-stub can be defined in order to obtain a sufficient over-strength with respect to the shear panel resistance, in this case an over-strength of the20% has been assumed:

$$F_{ep,Rd} = 1.2 \frac{M_{y,pz}}{(d_b - t_{bf})} \tag{11}$$

Making the hypothesis of T-stub failing according to a mechanism-1 it is possible to design the end-plate according to the following equation:

$$\frac{2 b_{eff} t_{ep}^2}{m} f_y = 1.2 \frac{M_{y,pz}}{(d_b - t_{bf})} \tag{12}$$

which leads to:

$$t_{ep} = \sqrt{\frac{1.2M_{y,pz}m}{(d_b - t_{bf})2b_{eff}f_y}} = \sqrt{\frac{1.2 \cdot 101000000 \cdot 37}{260 \cdot 154 \cdot 275}} = 20.18 \ mm \quad (13)$$

Therefore, as a simplification, a thickness equal to 20 mm has been adopted.

The ***bolts*** have been designed in order to guarantee a mechanism type-1. Assuming that the bolts are M20 made of 10.9 steel, the following limitation, assuring a mechanism type-1, has been verified:

$$t_{ep} \le \sqrt{\frac{4B_{Rd}nm}{b_{eff}f_y(m+2n)}} = \sqrt{\frac{4 \cdot 220500 \cdot 45 \cdot 37}{(154/2) \cdot 275(37+2 \cdot 45)}} = 23.4 \ mm \quad (14)$$

where b_{eff}*=154/2=77mm* is the effective width of the single bolt row.

Finally, in order to limit the plastic engagement of the ***column web panel*** in transverse compression, a sufficient over-strength has been provided also to this component, accounting also for buckling phenomena. With reference to the formulation provided by Eurocode 3, the buckling resistance of an unstiffened column web panel in compression can be determined as:

$$F_{cwc} = \omega k_{wc} \rho b_{eff,cwc} t_{cw} f_y \quad (15)$$

in which $\omega$is a factor accounting for the effects of shear interaction in the column web panel, k_{wc} is a reduction factor accounting for the influence of normal stress on the column web panel resistance, ρ provides the influence of the buckling phenomenon on the collapse strength, $b_{eff,cwc}$ is the effective width of the column web in transverse compression given by a spreading through at 45° through the end plate and by a 1:2.5 spreading through the column. Finally, t_{cw} is the column web thickness. The effective width of the column web panel in transverse compression for bolted end-plate connection is given by:

$$b_{eff,cwc} = t_{bf} + 2\sqrt{2}a + 5(t_{cf} + s) + s_p$$
$$= 10.2 + 2 \cdot 10 + 5 \cdot (15 + 18) + 40 = 235.2 \ mm \quad (16)$$

where s in case of rolled sections is the column flange-to-web root radius, s_p is the length obtained by a 45° spreading through the end-plate. The reduction factor for plate buckling $\rho$is defined starting from the definition of the plate slenderness:

$$\bar{\lambda}_p = 0.932\sqrt{\frac{b_{eff,cwc}d_{wc}f_y}{Et_{cw}^2}} = 0.932\sqrt{\frac{235.2 \cdot 134 \cdot 355}{210000 \cdot 9^2}} = 0.756 \quad (17)$$

where d_{wc} is the column web panel height. Being the plate slenderness greater than 0.72, the reduction factor ρ accounting for the buckling phenomenon is computed according to the Winter formula:

$$\rho = \frac{(\bar{\lambda}_p - 0.2)}{\bar{\lambda}_p^2} = \frac{(0.756 - 0.2)}{0.756^2} = 0.973 \quad (18)$$

Besides, the ω factor, which gives the influence of the shear interaction on the resistance of the web panel in transverse compression, is function of the parameter β. As already discussed βhas been assumed equal to 1, which is an assumption valid for external joints. The expression of the ωfactor for β=1 is given by Eurocode 3 as a function of the ratio between column web shear area (A_{vc}) and panel area in transverse compression.

$$\omega = \sqrt{\frac{1}{1 + 1.3\left(\frac{b_{eff,cwc}t_{cw}}{A_{vc}}\right)^2}} = \sqrt{\frac{1}{1 + 1.3\left(\frac{235.2 \cdot 9}{2483}\right)^2}} \cong 0.717 \quad (19)$$

In addition, the interaction factor accounting for normal stress effects, i.e. k_{wc}, can be assumed equal to 1, provided that normal stress at the column root radius does not exceed 70% of steel ultimate stress,. Thus the column web panel in transverse compression resistance is:

$$F_{cwc} = 0.717 \cdot 1 \cdot 0.973 \cdot 235.2 \cdot 9 \cdot 355 \ = 524252 \ N \quad (20)$$

Therefore, the over-strength level of the panel web in transverse compression is given by the ratio:

$$\frac{F_{cwc} \cdot (d_b - t_{bf})}{M_{y,pz}} = \frac{524252 \cdot 260}{101000000} \cong 1.35 \quad (21)$$

which is consider sufficient in order to prevent brittle failure modes.

Design of Specimen EEP-CYC 02

The second beam-to-column joint included in the experimental program has been designed with the purpose of investigating the ductility and energy dissipation capacity of an extended end-plate connection where the component mainly engaged in plastic range is the end-plate in bending. In this case, the exclusion of the components related to the column web panel requires the use of stiffeners, such as doubler plates and continuity plates. Specimen EEP-CYC 02 has been designed aiming to obtain the same resistance of specimen EEP-CYC 01, but relying on the ductility supply of the end-plate.

Design of the Weakest Joint Component

As for the previous specimen, the first component to be designed is the weakest component, i.e. the ***end-plate***. Afterwards, all the other components are designed to have sufficient over-strength aiming to avoid their plastic engagement. In order to provide to the connection a fixed value of the resistance and a sufficient ductility supply the T-stub is designed consequently. In particular, as reported successively, starting from these two design goals, it is possible to define the position of the bolts and the thickness of the plate.

The flexural resistance of the joint, assuming that the T-stub fails according to a mechanism type-1, can be determined as follows:

$$\frac{2b_{eff}t_{ep}^2}{m} f_y (d_b - t_{bf}) = M_{jR,d} = 100 \ kNm \quad (22)$$

where b_{eff} is the effective width of the single bolt row. It is worth noting that Eq.(22) is appliable provided that Eq.(14) is satisfied. In addition, aiming at the control of the plastic rotation supply, it can be evaluated as equal to the ratio between the plastic deformation of the T-stub modelling the bolt rows in tension and the lever arm:

$$\phi_u = \frac{\delta_{u,ep}}{\left(d_b - t_{bf}\right)} \tag{23}$$

According to Piluso *et al.* (2001), the ultimate plastic displacement of a T-stub failing according to type-1 mechanism can be computed as:

$$\delta_{u,ep} = \frac{Cm^2}{2t_{ep}} \tag{24}$$

where C is a constant depending on the material properties. The value C=0.1951 can be assumed for S275 steel grade [11]. Therefore, the plastic rotation supply can be computed as:

$$\phi_u = \frac{Cm^2}{2t_{ep}\left(d_b - t_{bf}\right)} \tag{25}$$

By imposing that M_j=100kNm (the same resistance of specimen EEP-CYC01) and ϕ_u=0.05 rad, Eq.(22) and Eq.(25) it is possible to define a system where the unknowns are the bolt location m and the end-plate thickness t_{ep}, whose solution provides:

$$m = \left[\frac{4M_{jR,d}\phi^2\left(d_b - t_{bf}\right)}{C^2 b_{eff} f_y}\right]^{1/3} = \left[\frac{2 \cdot 100000000 \cdot 0.05^2 \cdot 260}{0.1951^2 \cdot (154/2) \cdot 275}\right]^{1/3} = 54.4 \ mm \tag{26}$$

and:

$$t_{ep} = \frac{Cm^2}{2\phi_u\left(d_b - t_{bf}\right)} = \frac{0.1951 \cdot 54.4^2}{2 \cdot 0.05 \cdot 260} = 22.2mm \tag{27}$$

In addition, in order to assure a type-1 mechanism, Eq.(14) provides the following limitation to the end-plate thickness:

$$t_{ep} \le \sqrt{\frac{4B_{Rd}nm}{b_{eff} f_y (m+2n)}} = \sqrt{\frac{4 \cdot 220500 \cdot 40 \cdot 54.4}{(154/2) \cdot 275 \cdot (54.4 + 2 \cdot 40)}} = 25.96 \approx 26 \ mm \tag{28}$$

On the basis of the above results, dealing with specimen EEP-CYC02, an end-plate thickness t_{ep}=20 mm is chosen assuming a bolt location m=54 mm.

Design of Non-Dissipative Components

After the design of the weakest component of the joint, it is possible to design the components related to the column web zone. The ***shear panel*** resistance can be designed as already discussed with reference to EEP-CYC 01 specimen. In order to obtain a sufficient over strength degree, two 10 mm supplementary web plates have been adopted. By means of equations (4-9) and considering a full effectiveness of the supplementary web plates, the shear panel resistance can be computed as:

$$k_b = \frac{C_r EI_c}{\left[\left(d_b - t_{bf}\right)/2\right]^3} = \frac{5 \cdot 210000 \cdot 56960000}{\left[(270-10)/2\right]^3} = 27222576 \, N/mm \tag{29}$$

$$k_s = \frac{G(A_{vc} + R_f A_{dp})}{\left[\left(d_b - t_{bf}\right)/2\right]} = \frac{80769 \cdot (2483 + 3700)}{\left[(270-10)/2\right]} = 3841498 \, N/mm \tag{30}$$

$$K_e = \frac{k_b k_s}{k_b + k_s}\frac{\left(d_b - t_{bf}\right)}{2}\frac{\left(d_b - t_{bf}\right)}{\beta} = \frac{27222576 \cdot 3841498}{27222576 + 3841498}\frac{(270-10)^2}{2 \cdot 1} = 1.138 \cdot 10^{11} Nmm \tag{31}$$

$$M_{pz} = 1.137 \cdot 10^{11} \cdot 0.85 \cdot 0.00242 = 233.9 \cdot 10^6 Nmm \approx 234 \ kNm \tag{32}$$

Therefore, by adopting the supplementary web plates the resistance of the shear panel is greater than the joint design resistance of a factor greater than 2, so that it is expected that the panel zone remains in elastic range up to the failure of the end-plate in bending. Moreover, the use of a couple of continuity plates with a thickness equal to the beam flange thickness assures that the ***column web in tension and the column web in compression*** also remain in elastic range.

Design of Specimen EEP-DB-CYC 03

This is a full strength extended end-plate connection aimed at investigating the energy dissipation capacity of the connected beam. However, aiming to obtain the same flexural resistance of previous specimens, the reduced beam section (RBS) strategy, namely also ***"dog bone"***, has been adopted. The three parameters to be designed are the distance of the reduced section zone from the face of the column flange (a), the length of the reduced section zone (b) and the flange reduction width (c).

Design of the Weakest Component

The simple design procedure suggested in [31] has been adopted. In particular, it is suggested to use values of the two parameters a and b according to the following ranges:

$$0.5b_f \le a \le 0.75b_f \tag{33}$$

$$0.65d_f \le b \le 0.85d_f \tag{34}$$

last parameter to be considered is the amount of flange reduction (c) which controls the maximum bending moment at the RBS and, as consequence, the maximum moment at the face of the column flange. The value of c should be limited in order to obtain a moment at the column face in a range contained in the 85-100% of the beam cross section plastic moment. According to past experiences, [32] suggest to avoid the use of these kinds of connections for reductions greater than 50%. Therefore, c must not be greater than $0.25b_f$.

The design procedure usually is iterative, because the moment at the column face can be evaluated only after the choice of the three geometrical parameters, so that the fulfilment of suggested limits can be checked. In addition, the beam-column hierarchy criterion and the absence of shear mechanisms have to be checked. With reference to IPE 270 section of tested specimens, the design parameters have been identified after few iterations:

$$a = 70mm \ \ b = 180mm \ \ c = 22mm \tag{35}$$

In particular, the amount of flange reduction (c) has been dimensioned so that the plastic moment is equal to the joint resistance of the other specimens. In fact, the plastic moment of RBS is given by:

$$M_{pl,RBS} = W_{pl,RBS} f_y = \left[W_{pl,b} - 2ct_{bf}\left(d_b - t_{bf}\right)\right] f_y = \\ = \left[484000 - 2 \cdot 22 \cdot 10 \cdot (270 - 10)\right] \cdot 275 \\ = 101640000 Nmm \cong 101.6 \ kNm \quad (36)$$

Design of Non-Dissipative Components

The design of the other elements of the connection, which have to remain in elastic range, has been carried out taking in account two effects: the strain hardening of steel, considered by a 1.15 factor and the expected yield strength herein assumed equal to $1.13f_y$, resulting from a coefficient of variation equal to 0.07. Therefore, the expected resistance of RBS at its centre line can be evaluated as:

$$M_{RBS,E} = 1.15 W_{pl,RBS} f_{y,E} = 1.15 \cdot 369600 \cdot 1.13 \cdot 275 \\ = 132081180 Nmm \cong 132.1 \ kNm \quad (37)$$

Starting from the knowledge of the expected moment at the RBS centre, it is possible to evaluate the bending moment at the column face to check that it is contained in the stated limits and to design the end-plate and the shear panel in order remain in elastic range. To this scope it is necessary to evaluate the shear force acting at the RBS centreline, that is given by the ratio between the maximum moment expected at the reduced section zone given by Eq.(37) and the beam length up to the "dog-bone" centreline:

$$V_{RBS,E} = \frac{M_{RBS,E}}{\left(L_b - a - \frac{b}{2}\right)} = \frac{132081180}{\left(1460 - 70 - \frac{180}{2}\right)} \\ = 101601 N \cong 101.6 \ kN \quad (38)$$

where L_b is the beam length. Neglecting the end-plate thickness, the moment acting on the column face and the plastic moment of the beam can be evaluated by means of the following expressions:

$$M_c = M_{RBS,E} + V_{RBS,E}\left(a + \frac{b}{2}\right) = 132081180 + 101601\left(70 + \frac{180}{2}\right) = \\ = 148337340 Nmm \cong 148.3 \ kNm \quad (39)$$

$$M_b = W_{pl,b} f_{y,E} = 484000 \cdot 1.13 \cdot 275 \\ = 150403000 Nmm \cong 150.4 \ kNm \quad (40)$$

Therefore, being $M_c / M_b \cong 1$, the suggested limit 85%-100% is satisfied. It is easy to check that the strong column-weak beam requirement is also satisfied, being the sum of the plastic moments of columns, reduced to account for the influence of the axial load, greater than the bending moment M_c transmitted by the RBS to the column face.

In addition, according to FEMA 267A [33], the ***shear panel*** must be designed to withstand a shear action equal to 80% of the one corresponding to the maximum bending moment acting at the column face. Adopting for the ***panel zone*** the same structural detail of EEP-CYC 02 specimen, assuming a β factor equal to one, the following over-strength is obtained.

$$\frac{V_{R,sp}}{V_{S,sp}} = \frac{V_{R,sp}}{\frac{0.8 \cdot \sum M_c}{\left(d_b - t_{bf}\right)}} = \frac{900000}{\frac{0.8 \cdot 148337340}{(270 - 10)}} = 1.97 > 1 \quad (41)$$

Finally, the ***end-plate*** thickness can be evaluated, fixing the plate width b=154 mm (b_{eff}=77 mm), the bolt location m=33.5 mm and adopting M24 bolts of 10.9 class as follows:

$$t_{ep} = \sqrt{\frac{M_c m}{\left(d_b - t_{bf}\right) \cdot \left(2 b_{eff}\right) f_y}} = \sqrt{\frac{148337340 \cdot 33.5}{(270 - 10) \cdot (2 \cdot 77) \cdot 275}} = 21.24 mm \quad (42)$$

which gives the minimum thickness to be adopted to satisfy the resistance requirement, provided that mechanism type-1 is assured, and:

$$t_{ep} \le \sqrt{\frac{4 B_{Rd} nm}{b_{eff} f_y (m + 2n)}} = \sqrt{\frac{4 \cdot 317700 \cdot 35 \cdot 33.5}{77 \cdot 275 \cdot (33.5 + 2 \cdot 35)}} = 26.07 mm \quad (43)$$

providing the condition to be satisfied to assure type-1 mechanism. On the basis of the above results, an end-plate thickness equal to 25 mm has been chosen.

Design of Specimen TS-CYC 04/TS-CYC 05

This specimen is a traditional double tee connection. The design goal is, like in test EEP-CYC 02, to avoid the plastic engagement of the components related to the column web panel, i.e. the column web in tension and column web in compression and the panel zone in shear.

Design of the Weakest Component

The design of this joint can be carried out using the relationships already exploited for specimen EEP-CYC 02. Obviously, in this case the modelling by means of two separate ***bolted T-stubs*** is even more realistic. Also in this case the same flexural resistance of the other joints has been imposed requiring, in addition, a plastic rotation supply of about 0.08 rad so that the following geometrical requirements have been considered:

$$m = \left[\frac{2 M_{j,Rd} \phi^2 \left(d_b - t_{bf}\right)}{C^2 b f_y}\right]^{1/3} = \left[\frac{2 \cdot 100000000 \cdot 0.08^2 \cdot 260}{0.1951^2 \cdot 77 \cdot 275}\right]^{1/3} = 74.5 mm \quad (44)$$

$$t_{ep} = \frac{C m^2}{2\phi\left(d_b - t_{bf}\right)} = \frac{0.1951 \cdot 74.5^2}{2 \cdot 0.08 \cdot 260} = 26 mm \quad (45)$$

$$t_{ep} \le \sqrt{\frac{4 B_{Rd} nm}{b_{eff} f_y (m + 2n)}} = \sqrt{\frac{4 \cdot 220500 \cdot 40 \cdot 74.5}{77 \cdot 275 \cdot (74.5 + 2 \cdot 40)}} = 28.3 mm \quad (46)$$

A plate thickness equal to 25 mm and a bolt location with m equal to 73 mm have been chosen to respect ductility requirement. The two T-stub elements have been connected through the ***webs*** to the beam flanges by means of eight M20 bolts. The ultimate strength of such connection according to Eurocode 3, is given by:

$$F = n_b \alpha_v f_{ub} A = 8 \cdot 0.5 \cdot 1000 \cdot 245 \\ = 980000 N \ge \frac{M_{j,Rd}}{\left(d_b - t_{bf}\right)} = 384615 N \quad (47)$$

The panel zone has been over-strengthened as in the other cases. Specimen TS-CYC 05 has been designed in order to have a resistance similar to specimen TS-CYC 04 but with an asymmetrical position of the bolt rows with respect to the web in order to increase their ductility supply.

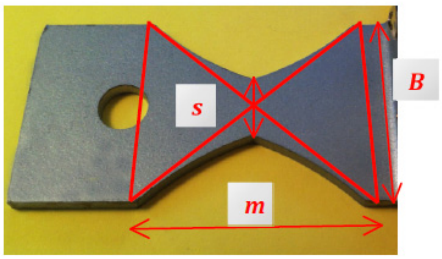

Fig. (4). Hourglass T-stub.

Design of Specimens TSJ-XS CYC 06/TSJ-XS CYC 07

Tested specimens are two dissipative double split tee connection which are realized by substituting the classical rectangular T-stubs with a couple of X-shaped T-stubs [18, 34, 35]. This particular type of T-stub is conceived in order to work as a yielding damper adopting the basic concepts governing the behaviour of plates working under double curvature, such as ADAS (Added Damping and Stiffness) devices. In particular, as demonstrated by [34] by properly tapering the flange plate in the region between the T-stub web and the bolt, a T-stub with high dissipative capacities can be developed. In fact, an hourglass shape of the T-stub flange allows to obtainthe contemporary yielding in all the plate sections which leads to a uniform spread along the whole plate, improving ductility supply.

A wide experimental analysis has already been carried out on dissipative T-stubs in order to evaluate their dissipative capacity [34] (Fig. **4**). In particular, in order to completely point out the different plastic behaviour under cyclic loads of the hourglass T-stubs and of the rectangular T-stubs, low cycle fatigue curves have been carried out [36] pointing out the significant improvement of the energy dissipation capacity provided by bolted hourglass T-stubs Fig. (**5**).

Starting from the above results, in order to show the benefits related to the adoption of the X-shaped T-stubs in connections, an experimental program on DST joints equipped with hourglass T-stub flanges has been carried out [37].

As for specimens TS-CYC 04 and TS-CYC 05, aiming to involve the connection in the energy dissipation, the design of the DST connections has been performed by imposing that the weakest joint components are the bolted T-stubs while the other connecting elements have been designed with a sufficient overstrength aiming to avoid their plastic engagement. For the dissipative T-stubs, the rules already proposed by [34] for predicting stiffness and resistance, have been adopted.

In particular, in order to make a direct comparison with ajointwith classical T-stubs, tests TSJ-XS CYC 06/07 have been designed in order to provide a flexural resistance and stiffness equal to that of joint TS-CYC 04, i.e. 100 kNm and 324.7 kN/mm respectively. As the design requirements are two, i.e. stiffness and resistance, damper width and length are assumed as design parameters, while thickness of the flange plate is assumed equal to 25 mm. Provided that the

T-stub in tension is the weakest joint component failing according to type-1 mechanism, the following expression can be written:

$$M_{jR,d} = \frac{2\eta B_{eff} t_{ep}^2}{m} f_y \left(d_b - t_{bf}\right) = 100 \ kNm \tag{48}$$

where f_y is the material yield strength, d_b is the beam depth and t_{bf} is the thickness of the beam flangeη is a factor accounting for the reduction of the resistance due to moment-shear interaction [37]. In addition, considering the equation given in [34], defining the stiffness of the hourglass T-stub, the following design condition can be written:

$$0{,}25\frac{EB_{eff} t_{ep}^3}{m^3} = S_{jR,d} = 324737 \ \ N/mm \tag{49}$$

by solving the system of equation defined by Eqs.52 and 53, the flange plate geometry has been defined as follows:

$$\begin{cases} \eta = 0.827 \quad ; \quad s/B = 0.325 \\ m = \sqrt{\dfrac{0.25 \cdot E \cdot t \cdot M_{j,Rd}}{2\eta \cdot f_y \left(d_b - t_{bf}\right)}} = \sqrt{\dfrac{0.25 \cdot 210000 \cdot 25 \cdot 100000000}{20.827 \cdot 275(270-10)}} = 58.45 \cong 59 mm \\ B_{eff} = \dfrac{S_{jR,d} m^3}{0.25 \cdot E \cdot t^3} = \dfrac{324737 \cdot 58.45^3}{0.25 \cdot 210000 \cdot 25^3} = 79.77 mm \\ B = \dfrac{B_{eff}}{e \cdot \left(\dfrac{s}{B}\right) \ln\left(\dfrac{B}{s}\right)} = 80.34 \cong 81 mm \end{cases} \tag{50}$$

where s is the width of the hourglass T-stub at the mid-section, B is the width at the clamped section and B_{eff} is the value of the effective width proposed by [34].

As already done before the bolts have been designed in order to assure a type-1 mechanism verifying the following condition:

$$\text{TSJ-XS CYC06} \quad t_{ep} \le \sqrt{\frac{4B_{Rd} nm}{b_{eff} f_y (m+2n)}} = \sqrt{\frac{4 \cdot 220500 \cdot 50 \cdot 59}{(81) \cdot 275(59+2 \cdot 50)}} = 27 \ mm \tag{51}$$

$$\text{TSJ-XS CYC07} \quad t_{ep} \le \sqrt{\frac{4B_{Rd} nm}{b_{eff} f_y (m+2n)}} = \sqrt{\frac{4 \cdot 505000 \cdot 50 \cdot 59}{(81) \cdot 275(59+2 \cdot 50)}} = 41 \ mm \tag{52}$$

Thereforethe T-stub elements of the two joints have been fastened to the column through bolts M20 and M30 class 10.9 respectively. In addition, in order to avoid the engagement of the ***components on the column***, as for the other stiffened specimens, continuity plates and supplementary web plates have been adopted.

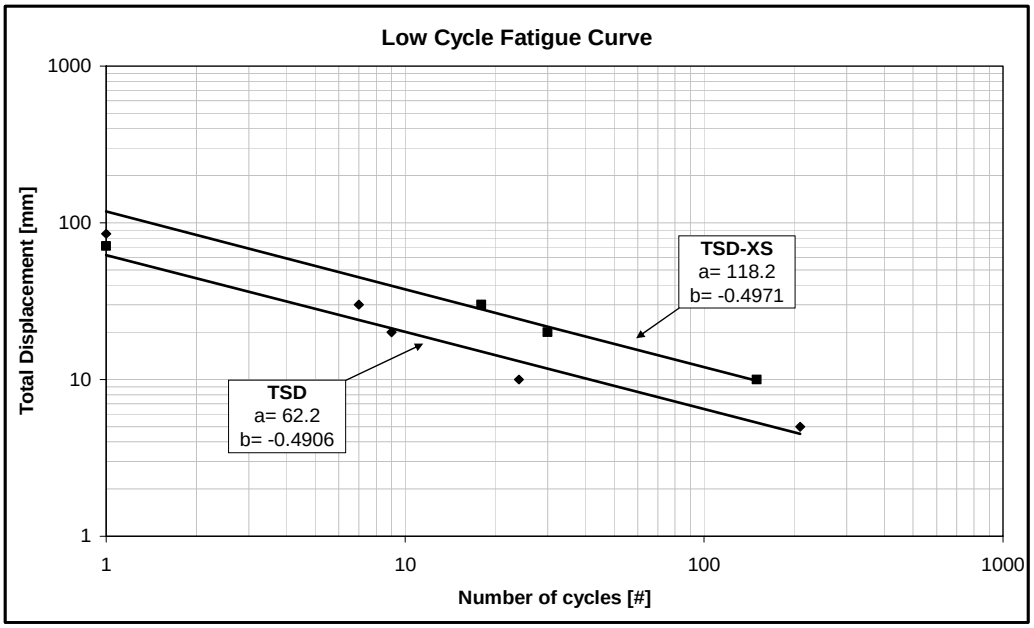

Fig. (5). Low-cycle fatigue curves of rectangular (TSD) and hourglass (TSD-XS) T-stubs [34].

Design of Specimens TSJ-M1-CYC08/TSJ-M2-CYC09/TSJ-M2-DS-CYC10/TSJ-B-CYC11

As an alternative to classical joints, in [38, 39] another innovative connection has been proposed, based on the application of friction dampers to beam-to-column connections [40, 41]. In particular, the proposed innovative joint is realized by modifying the classical DST joint detail by a adding a friction pad in between the T-stub stem and the beam flange, which has to be designed in order to prevent its slippage under serviceability limit states and to be activated under severe seismic loading conditions, according to the basic principle of the passive control techniques [42-44]. With the proposed approach the friction mechanism is used to dissipate the seismic input energy and the component method is applied in order to prevent the plastic engagement of other joint components. In order to characterize the behaviour of the main source of energy dissipation capacity component (the friction damper pres-stressed with high strength bolts), tests on different materials have been carried out in order to determine the values of the friction coefficient to be employed in the design.

The tests have been carried out on a sub-assemblage composed bya layer of friction material that has been placed in between plates made of S275 steel Fig. (**6**). In order to allow the relative movement of the steel on the interposed friction material, one of the inner plates has been realized with slotted holes.

Conversely, the other inner and the two outer plates have been realized with circular holes. The clamping force has been applied by means of 16 M20 bolts 10.9 class [5] and the holes have been drilled with a 21 mm drill bit. Aiming to evaluate the magnitude of the friction coefficient and the cyclic response, several different layouts of the sub-assemblage have been considered varying three parameters: the interface, the tightening torque and the number of tightened bolts,investigating the friction characteristics of the following three interfaces:

- Brass on steel;
- Rubber material M1 on steel;
- Rubber material M2 on steel.

The results of the experimental campaign on the sub-assemblage have provided the values of the friction coefficient for all the considered interfaces. In particular, starting from the test results, the friction coefficients have been determined as:

$$\mu = \frac{F}{m\, n\, N_b} \tag{53}$$

where m is the number of surfaces in contact, n is the number of bolts, N_b is the bolt preloading force and F is the sliding force [20].

Starting from the behavior of the sub-assemblage the design of dissipative DST connections with friction pads has been performed (Fig. (**7**), Table **2**). In particular, the use of slotted holes on the tee stem and the location of a friction pad between the stem and the beam flange allows to provide the connection with a friction damper Fig. (**8**). The slip resistance of the friction damper has to be designed so that the connection is able to withstand a bending moment less than the beam plastic resistance. Therefore, the yielding of the beam end is prevented and the beam-to-column connection results free from damage, provided that the connection components are designed to exhibit a resistance greater than the slip resistance of the friction damper. In order to control the slip resistance at the interface, analogously with the sub-assemblage already studied, the interface is pre-stressed by means of high strength bolts whose tightening torque is properly calibrated according to the adopted design criteria.

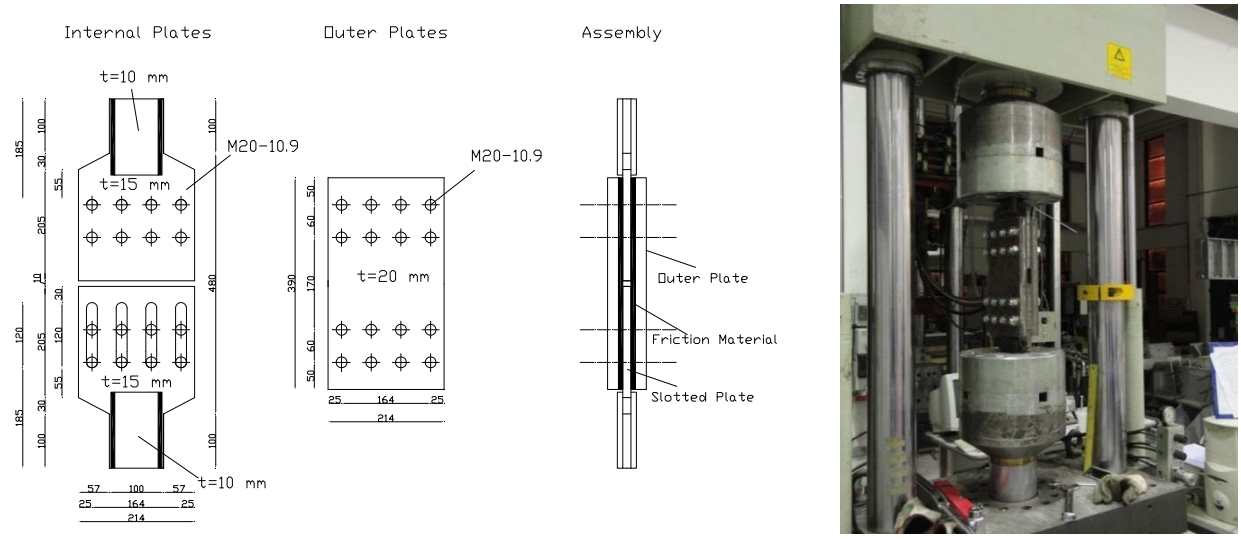

Fig. (6). Scheme of the adopted sub-assemblage.

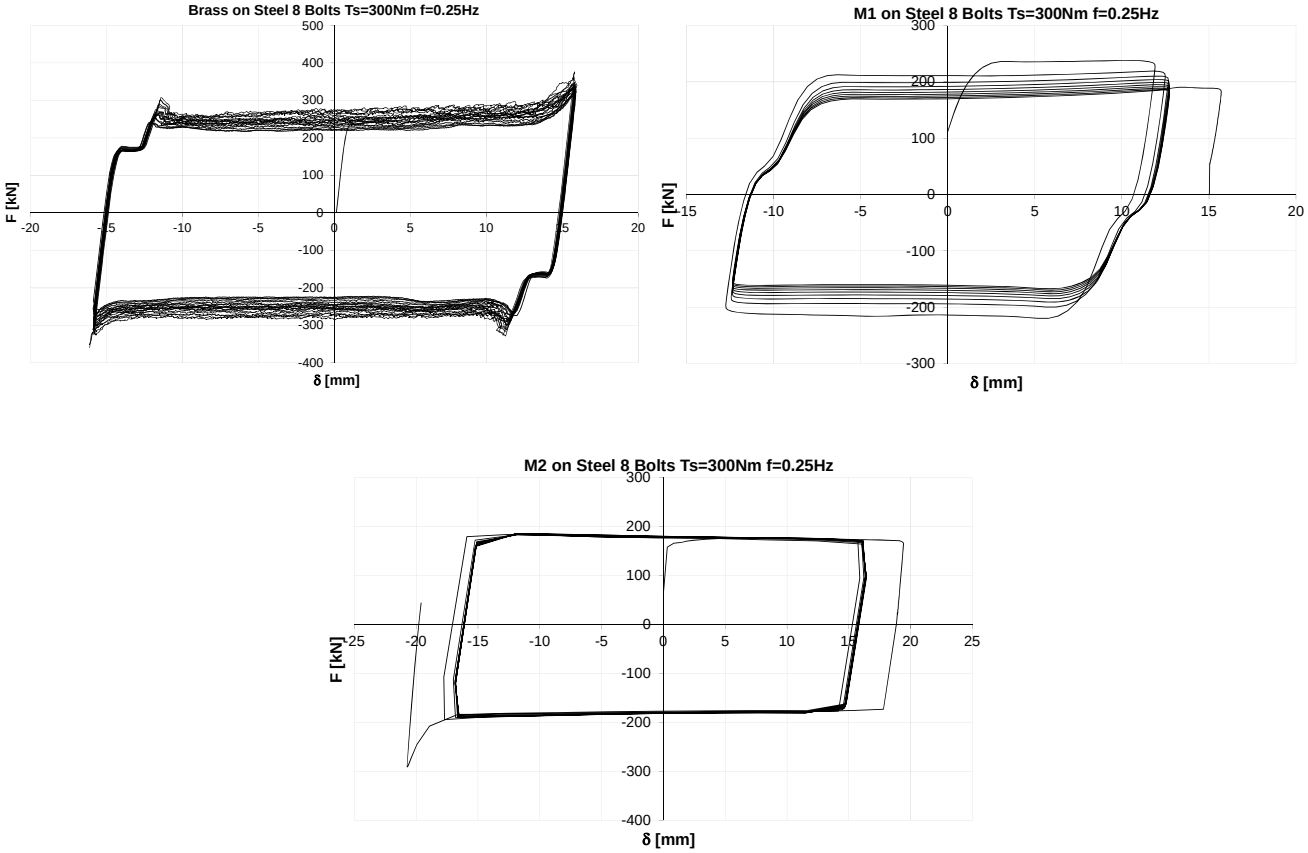

Fig. (7). Cyclic response of friction materials.

The design resistance is the same assumed for joint TS-CYC 04, i.e. $M_{Rd} = 100\ kNm$ All the joint components, with the only exception of the friction pad, have to be designed with sufficient overstrength to avoid their yielding.

In particular, the ***panel zone*** has been designed adopting the same detail previously specified for joint, obtaining, therefore, a proper over-strength.In order to prevent the yielding of the ***T-stubs***, they have been designed to

Table 2. Values of the friction coefficientsto be used in design.

Inteface	μ
Brass on Steel	0.200
M1 on Steel	0.201
M2 on Steel	0.180

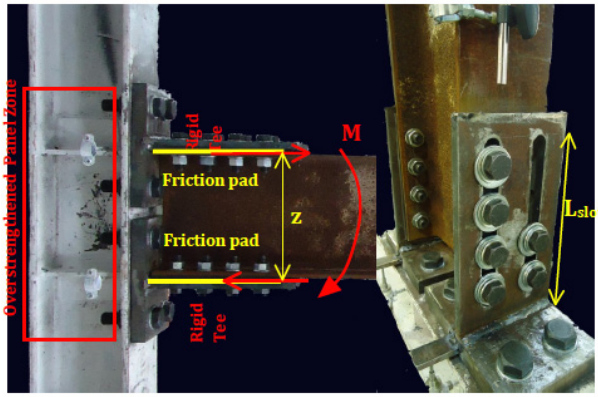

Fig. (8). Concept of the tested joint.

withstand a tensile force equal to the design bending moment divided by the lever arm multiplied for an over-strength factor equal to 1.5:

$$F_{T-stub} = \frac{M_d}{z} = 1.5\frac{100000}{286} = 530 \ kN \quad (54)$$

where z is evaluated as the distance between the friction pads. Assuming that the T-stub fails according to mechanism type-1 of Eurocode 3, its plastic resistance can be determined as the sum of the plastic resistances of the two bolt rows which, in the present case, are characterized by different values of the distance m between the bolt row and the T-stub web:

$$F_{T-stub} = \frac{b_{eff}t_p^2}{m_1}f_y + \frac{b_{eff}t_p^2}{m_2}f_y \quad (55)$$

where, according to the T-stub geometry, $b_{eff}$is the effective width assumed as equal to one half of the total T-stub width (85.5 mm), m_1 is equal to 63 mm, m_2 is equal to 78.9 mm, t_p is the plate thickness and f_y is the yield strength of the plate equal to 275 MPa. Therefore, t_p can be determined as:

$$t_p = \sqrt{\frac{F_{T-stub}\left(\frac{m_1 m_2}{m_1+m_2}\right)}{b_{eff}f_y}} = \sqrt{\frac{530000\left(\frac{63\cdot 78.9}{63+78.9}\right)}{85.5\cdot 275}} = 28.1\,mm \quad (56)$$

As a consequence, a 30 mm thick plate has been selected for the T-stub flange. The bolts fastening the T-stub flange to the column have been designed in order to guarantee a type-1 collapse mechanism. In particular, according to the component method it is well known that this condition is satisfied if the following inequalities are verified:

$$\frac{b_{eff}t_p^2 f_y}{2B_{Rd}m_1} \le \frac{2n/m_1}{1+2n/m_1} \quad \frac{b_{eff}t_p^2 f_y}{2B_{Rd}m_2} \le \frac{2n/m_2}{1+2n/m_2} \quad (57)$$

where n is the distance between the bolts axis and the free edge of the T-stub flange, assumed equal to 45 mm. By means of Eq. (12), the design of the bolts has been carried out as follows:

$$B_{Rd} \ge \frac{(1+n/m_1)b_{eff}t_p^2 f_y}{4n} = 201.5 \ kN$$

$$B_{Rd} \ge \frac{(1+n/m_2)b_{eff}t_p^2 f_y}{4n} = 184.6 \ kN \quad (58)$$

M27 bolts made of 10.9 class have been adopted.

Dealing with ***friction dampers***, they have been designed in order to allow the slippage of the friction pad on the T-stub web. To this scope, the length of the slotted holes has been properly designed as a function of the desired value of the joint rotation capacity by means of the following equation:

$$L_{slot} = (n_{br}-1)p + d_b + 2\varphi z \quad (59)$$

where d_b is the bolt diameter, n_{br} is the number of bolt rows used to fasten the web of the T-stub to the beam flange, p is the bolt pitch and ϕ is the design value of the joint rotation capacity. By adopting eight M20 bolts located according to four rows, with a spacing equal to 60 mm and by assuming a design joint rotation equal to +/- 70 mrad, it follows:

$$L_{slot} = (4-1)60 + 20 + 2\cdot 0.07\cdot 286 = 240 \text{ mm} \quad (60)$$

The bolt preloading level has been assumed for the different joints as equal to 460 Nm. The details of all the specimens are reported in Fig. (**9**).

3.2. Experimental Results

In the following the main results of the experimental analysis are reported, evidencing the accuracy of the design procedures.

Description of Test EEP-CYC 01

According to the design criterion, specimen EEP-CYC 01 (Fig. **10a**) has exhibited shear panel yielding since the first cycles. In fact, the formation of 45° yield lines on the panel zone has been immediately observed by means of the white wash that was used to paint the joint. The failure condition has been attained due to the collapse of the welds connecting the beam flange to the end-plate.

This failure mode, due to the stress concentration arising in the welds in the central zone (Fig. **10b**), is typical of end-plate or welded joints when continuity plates are omitted. According to the adopted hierarchy criterion, no participation of other joint components has been observed during the test. The results delivered in (Fig. **17**) show that the cyclic

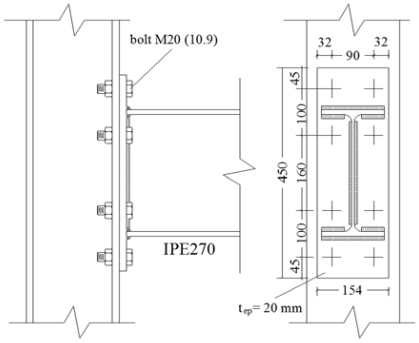

EEP-CYC 01

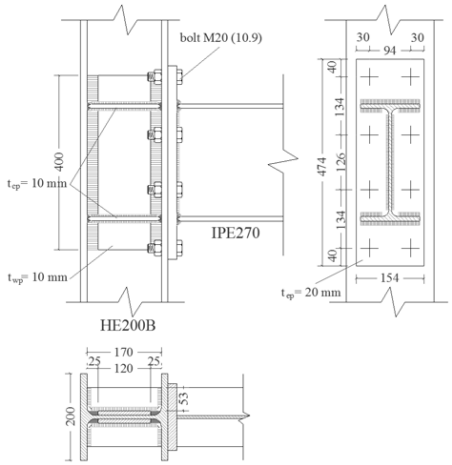

EEP-CYC 02

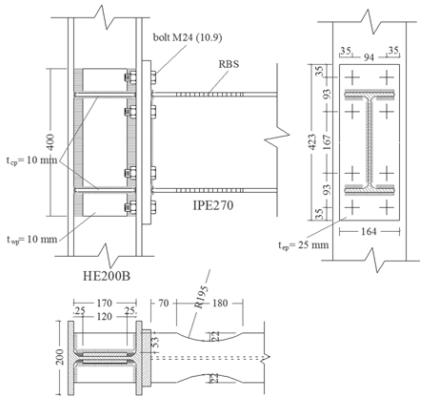

EEP-DB CYC 03

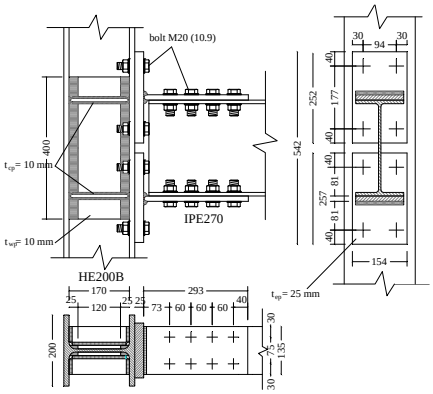

TS-CYC 04

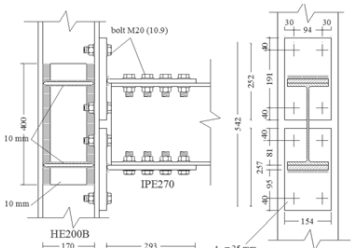

TS- CYC 05

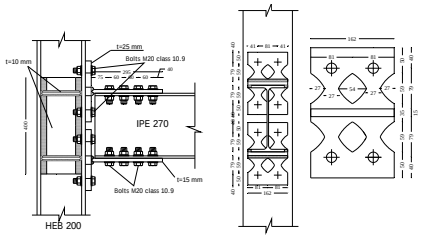

TSJ-XS-CYC 06

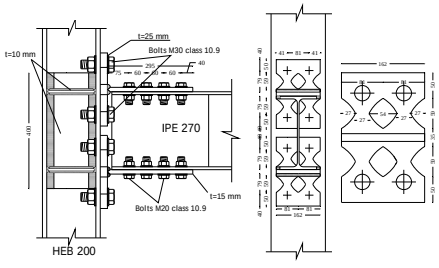

TSJ-XS-CYC 07

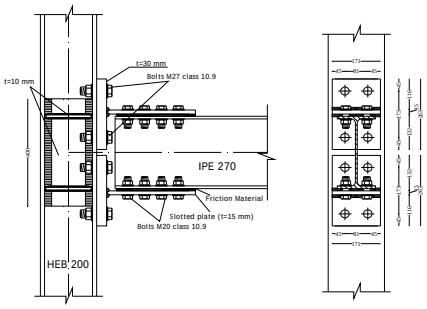

TSJ-M1 CYC08/TSJ-M2 CYC09/TSJ-M2-DS CYC10 and TSJ-B CYC11

Fig. (9). Geometry of the tested specimens.

Fig. (10). a) Yielding of the panel zone **b**) Failure of the weld.

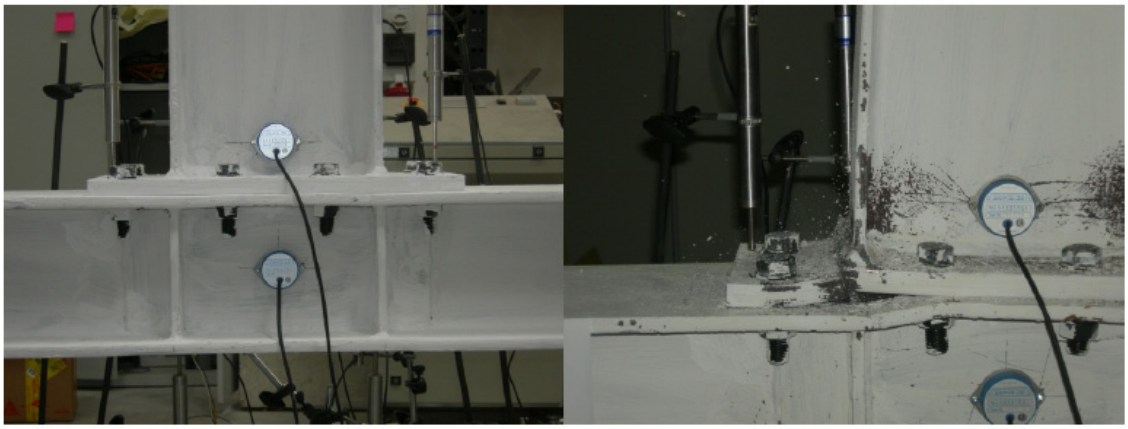

Fig. (11). a) Specimen before the test **b**) Failure of the end-plate.

response of this joint quite stable up to failure with a very low progressive stiffness degradation, evidencing the good ability of the connection to dissipate energy.

Description of Test EEP-CYC 02

Specimen EEP-CYC 02 has been designed in order to concentrate the energy dissipation in the end-plate components (Fig. **11a**). In this case, the observed behaviour is completely different from the one of the previous joint, in fact analyzing both the moment-rotation response of the whole joint and the displacement response monitored with the LVDT located on the shear panel during the test, it has been recognized that due to the presence of the doubler plates, the shear panel almost remains in elastic range. Similarly, due to the presence of continuity plates, the column web in tension and compression does not provide significant energy dissipation.

The only components involved in the energy dissipation, as expected, are the left end-plate and the right end-plate T-stub which also govern the shape of the moment-rotation cyclic response of the joint where some pinching can be observed. The joint collapse occurred due to the fracture of the end-plate in the extended part close to the column flange (Fig. **11b**). The residual load carrying capacity occurring at the end of the test is due to the final behaviour like a flush end-plate connection.

Description of Test EEP-DB-CYC 03

The aim of specimen EEP-DB-CYC 03 is to show the dissipation capacity and ductility of a full strength joint, providing a comparison with the previously tested partial strength joints. The adopted design criteria have been presented in the previous section, pointing out the strategy adopted in order to assure that all the components remain in elastic range concentrating yielding in a reduced beam section zone far from the connection zone.

The displacements measured by LVDT registrations confirmed that the connection component contribution is negligible, in fact yielding has been concentrated only in the reduced beam section zone Fig. (**12**). The failure mechanism is the one typical of steel members with I section shape. In particular, after yielding of flanges and web and the attainment of the maximum flexural resistance, flange local buckling occurs accompanied by beam web buckling due to compatibility between flange and web out-of-plane displacements.

The shape of the cycles of the whole joint is, as well known from the technical literature, wide and stable, providing a very high energy dissipation capacity and significant plastic rotation supply Fig. (**17**).

Description of test TS-CYC 04/TS-CYC 05

TS-CYC 04 and TS-CYC 05 are double tee connection where the only elements involved in the energy dissipation

are the top and bottom T-stubs, having four bolts, which are alternatively subjected to tension and compression. The behaviour of the two connections has been analogous.

Fig. (12). Failure of the reduced section zone.

As expected the joints have provided high rotational capacity and energy dissipation Fig. (**17**). The shape of the hysteresis loops of double tee connections, designed to dissipate energy in the flanges of tee elements, is similar to the one of extended end-plate connections designed to dissipate energy in the end-plate, because both of them are obviously affected by pinching phenomena. The main advantage of this kind of connection, provided that the weakest joint component is constituted by the tee elements, is due to the fact that the beam end does not exhibit any yielding, so that after a seismic event only the tee elements have to be substituted.

The behaviour during the tests has been the one expected according to the design based on the component approach. In particular, the plastic engagement of the T-stubs has been observed with the development of plastic hinges at the bolt rows (Fig. **13a**,**b**).

Failure occurred due to the development of cracks located in the heat affected zone of the tee flange due to the welded connection with the tee web. These cracks are initially located in a position corresponding to the projection of the bolt axis perpendicular to the tee web. As far as the number of cycles increases these cracks propagate both toward the inner part of the flange and toward the flange edges leading to complete fracture of the flange (Fig. **13a**,**b**).

Description of Test TSJ-XS-CYC 06

The behavior of the specimen during the test has been the one expected according to the design criteria. In fact, only the plastic engagement of T-stubs has been observed with development of plasticization in the dissipative elements Fig. (**14**). The shape of the hysteresis loops is similar to that exhibited by joint TS-CYC 04. In fact, significant pinching phenomena, mainly due to the bolt plastic deformation, have been evidenced Fig. (**17**).

Joint TSJ-XS-CYC06 exhibited lower plastic rotation supply and less energy dissipated at collapse compared to the case of joint TS-CYC 04. In fact, in contrast with the prediction, in case of joint TSJ-XS-CYC 06, even though bolts were designed to allow full plasticization of the plate, collapse condition was reached due to their premature fracture, which limited the rotational capacity of dissipative T-stubs. In particular, premature collapse of bolts was caused by the flexural effects due to compatibility requirements with the plate plastic deformations. In fact, the influence of bending moment on bolts ultimate resistance is an aspect neglected in classical T-stub theory and represents an approximation that, as in the examined case, can lead to a poor prediction of the T-stub ductility.

Description of Test TSJ-XS-CYC 07

Even though only bolts diameter differentiates joint TSJ-XS-CYC 06 and TSJ-XS-CYC 07 some substantial differences can be evidenced in the hysteretic behavior. Test has still been characterized by pinching phenomena, but did non exhibit strength degradation up to failure, which arose at the 44^{th} cycle at ultimate rotation of 10% with the formation of a crack on the flange plate Fig. (**15**).

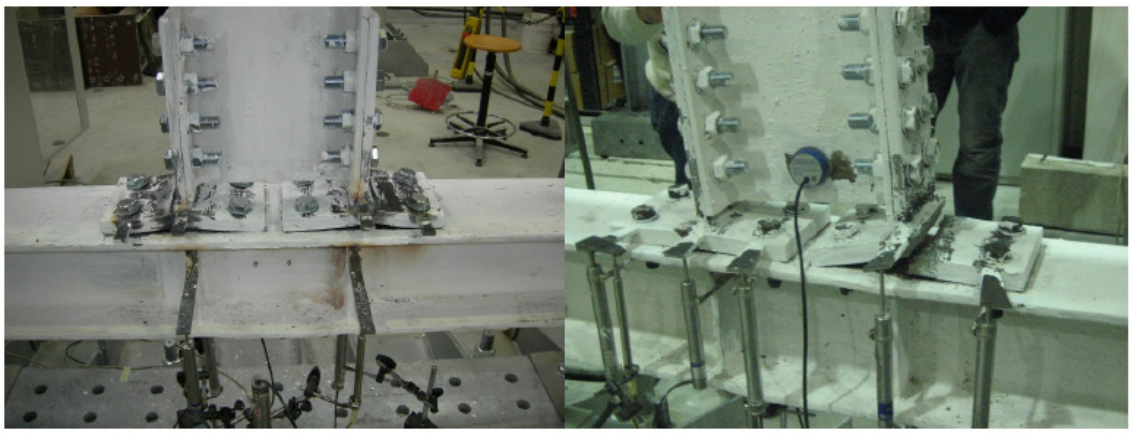

Fig. (13). a) Specimen at failure (TS-CYC 04); **b)** Specimen at failure (TS-CYC 05).

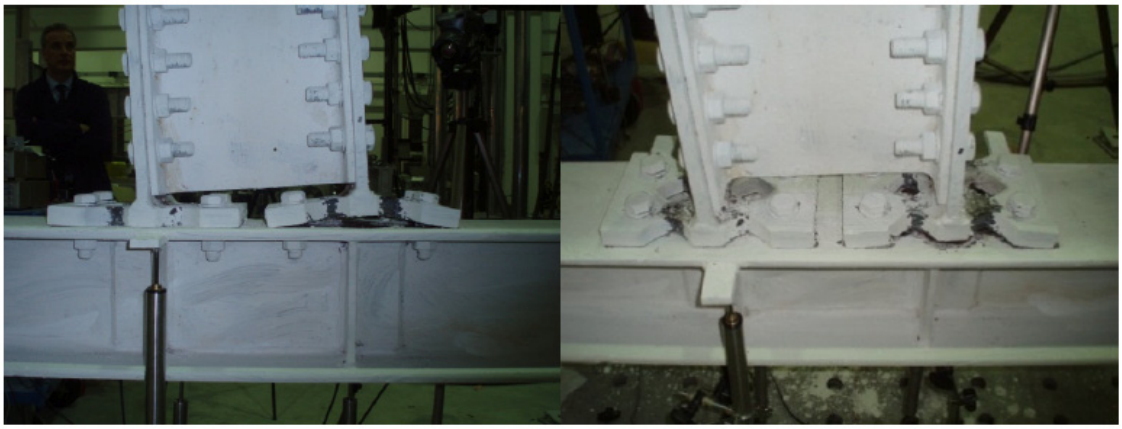

Fig. (14). a) Plastic engagement of the X-shaped T-stub; **b)**Specimen at failure.

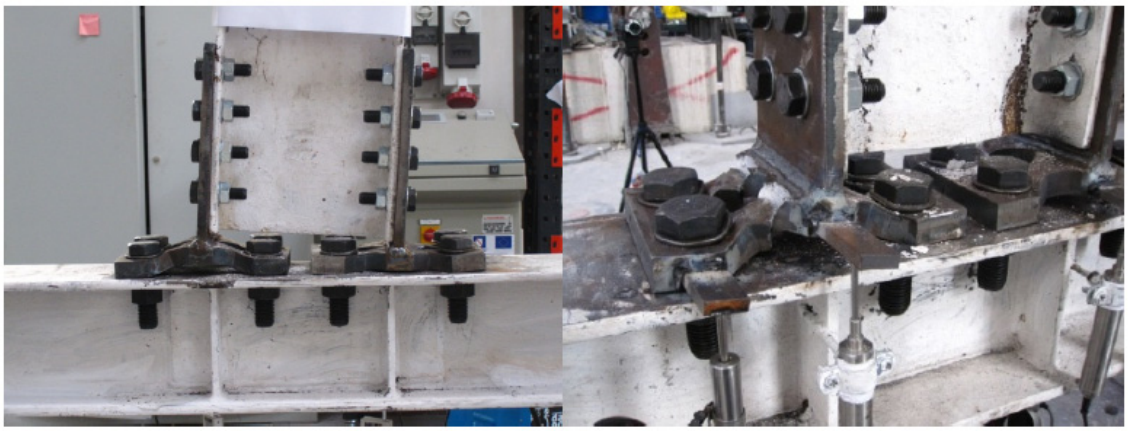

Fig. (15). a) Specimen during the test; **b)** Specimen at failure.

As expected, during this test the only components engaged in plastic range have been the hourglass T-stubs in tension and compression. Components on the column panel have not been significantly involved in the dissipation mechanism. Failure condition has been reached after the full development of the cyclic ductility supply of the steel dampers. Collapse occurred due to the formation of a crack, which started in the heat-affected zone and then propagated through the plate following a circular shaped pattern. This particular failure mode, which differentiates the behavior at collapse of hourglass T-stubs from those of classical T-stubs, whose failure is usually characterized by the formation of a straight crack in correspondence of welds, may found a theoretical justification in the results obtained in previous paragraph. In fact, in case of dissipative T-stubs, the section of minimum resistance where first plasticization occurs is not necessarily located in correspondence of the section of maximum width. As far as the bending moment is linear with point of zero at the mid-section and shear is constant along the plate, due to the moment-shear interaction, the section of minimum resistance, depending on the plate geometry, can be in general located somewhere in between T-stub web and damper centerline.

Description of Tests on the Friction Joints

As expected on the basis of the design criteria adopted, in all the experimental tests on joints equipped with friction dampers there has not been any damage of the joint components, but only the wearing of the friction pads. Therefore, a very important result coming from the experimental program is the confirmation that this connection typology can be subjected to repeated cyclic rotation histories, i.e. to repeated earthquakes, by only substituting the friction pads, if needed, and by tightening again the bolts to reach the desired preloading level. In addition, in all the tests the rotation demand applied to the joint has been completely due to the slippage of the friction material on the T-stub web).

The experimental results are in line with the results pointed out in the tests on the friction interfaces pointing out that, as expected, the cyclic behavior of the joint is mainly governed by the cyclic behaviour of the friction damper. In test ***TSJ-M1-CYC08***, at low force values the joint exhibited an elastic behavior while, when a bending moment level approximately equal to the design one is reached, the slippage of the friction dampers starts. However, the cyclic behaviour of this joint has been quite poor, mainly due to the low tensile strength of the friction material which failed at a value of the rotation amplitude relatively low, equal to about 20 mrad. In particular, the joint failure occurred due to the collapse of the rubber plate in the zone weakened by the holes. Conversely, the joint equipped with friction pads made of material (***M2***) exhibited a better response. In particular, also in this case, the hysteretic behavior of the joint has been mainly governed by the response of the friction dampers

obtaining, as already observed in tests on the joint component, wide and stable hysteretic loops. For bending moment levels less than the design resistance, the cyclic behaviour has been characterized by loading and unloading elastic branches.

After the attainment of a bending moment value approximately equal to 100 kNm, the slippage of the friction dampers has occurred. In this phase, the joint hysteretic response has been characterized by cycles with a parallelogram shape. It is useful to note, from the comparison with the response of tests on friction dampers, that the shape of the hysteresis cycle of the friction DST joint differs from that observed during the uni-axial tension test. This difference is mainly due to the role played by the beam rotation in the kinematic mechanism. In fact, the beam rotation causes two effects that give rise to an increase of the bending moment as far as the beam rotation increases. On one hand, there is an increase of the local pressure on the friction pads due to the reaction force provided by the T-stub webs that behave in a way similar to a pocket foundation. On the other hand, minor yielding of the tee stems at the web-to-flange attachment contributes to the total bending resistance of the joint. Both of these effects lead to the hardening behaviour experimentally observed. Moreover, the results of test ***TSJ-M2-CYC09*** show that, at high rotation amplitudes, slight strength and stiffness degradation occurs, probably due to the consumption of the friction pads during the sliding motion.

Starting from the behaviour previously observed, another test with the same layout but adopting disc springs interposed between the bolt head and the tee web plate has been carried out (***TSJ-M2-DS-CYC10***). In this way, it was expected that the pinching and degradation behaviour due to the wearing of the friction material observed during test TSJ-M2-CYC09 is overcome. This particular type of washer is a high resistance cone shaped annular steel disc spring which has a behaviour very similar to a classical spring [45, 46]. In fact, it flattens when compressed and returns to its original shape if compression loading is released. In this way, as the friction material wears, leading to the partial loss of bolt preload, the disc spring restores the force by maintaining the bolt shank in tension. The results of test TSJ-M2-DS-CYC10 demonstrate the effectiveness of the adopted disc springs. In fact, the obtained cyclic behaviour is very similar to that exhibited by specimen TSJ-M2-CYC09, but a higher dissipation capacity and lower strength and stiffness degradation was obtained Fig. (**17**).

Test on Brass ***TSJ-B-CYC11*** (Fig. **16**) also exhibited a satisfactory behaviour in terms of shape of the cyclic response. In fact, the cycles obtained have been very stable also at high values of the plastic rotation. Nevertheless, a value of the bending moment less than the design value equal to 100 kNm was obtained. This result can be justified on the base of the results obtained on the subassemblage [20]. In fact, in case of brass on steel interface the value of the static friction coefficient is much lower than the dynamic one and, as a consequence, a bending moment lower than the expected one has been obtained Fig. (**17**).

Energetic Comparison

All the tested specimens exhibited almost the same flexural strength, as desired, and provided energy dissipation mainly in the weakest component according to the adopted design criteria. Therefore, experimental test results confirmed that the component approach can be a powerful tool, even in the framework of seismic design of steel structures, allowing the selection of dissipative elements and the application of hierarchy criteria to design the joint components which have to remain in elastic range.

The comparison between the different experimental tests in terms of energy dissipation allows to make some considerations. In particular, in (Fig. **18**) the values of the energy dissipated by the different joints versus the number of cycles are reported. The highest energy dissipation capacity has been exhibited by specimen EEP-DB-CYC 03 adopting the RBS strategy, revealing that generally joints are able to provide an energy dissipation supply that it is always lower than steel members. Connections providing the highest energy dissipation capacity are those engaging in plastic range the column web panel (EEP-CYC 01) and the friction joint employing disc springs. In these cases a reduction of about 20%

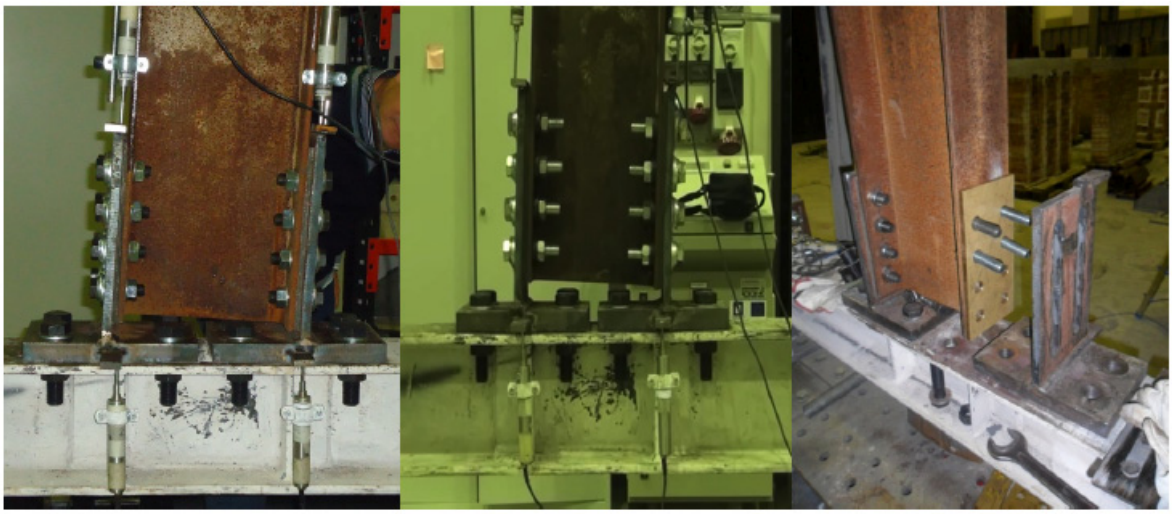

Fig. (16). Tests TSJ-M2-CYC09 (left) TSJ-M2-DS-CYC10 (middle), TSJ-B-CYC11 (right).

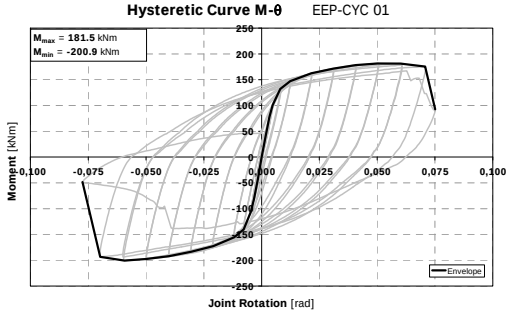

EEP-CYC 01

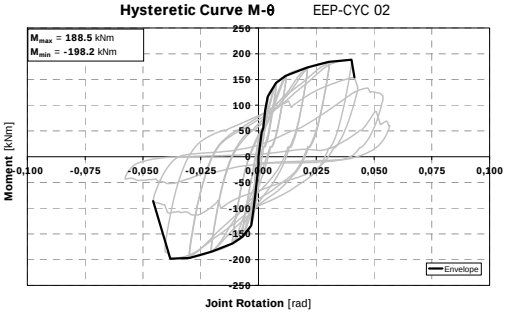

EEP-CYC 02

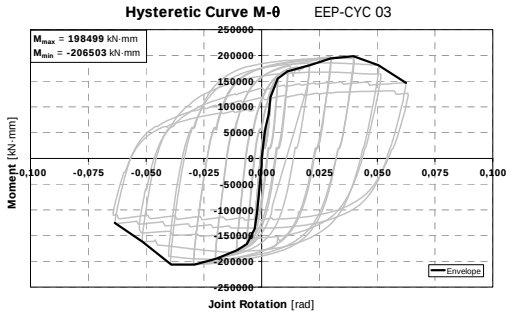

EEP-DB CYC 03

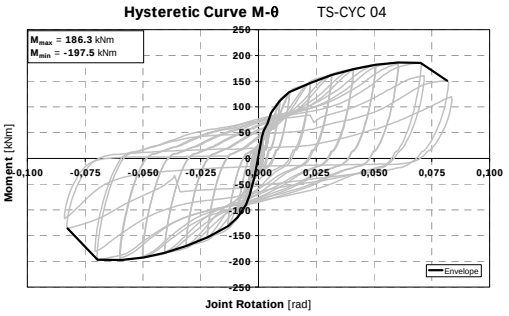

TS-CYC 04

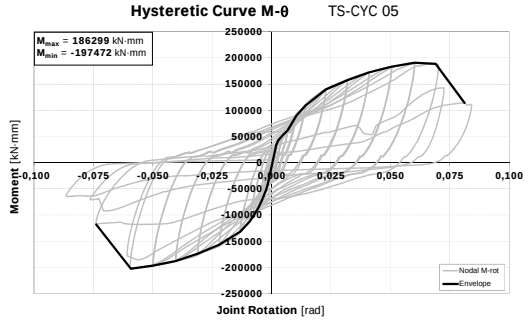

TS-CYC 05

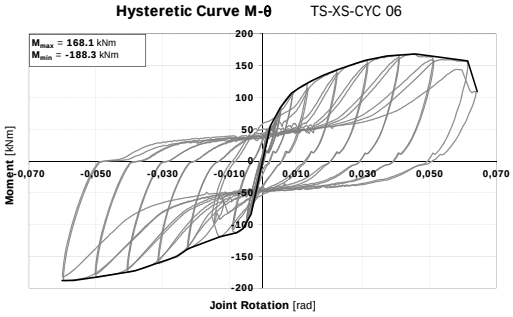

TSJ-XS-CYC 06

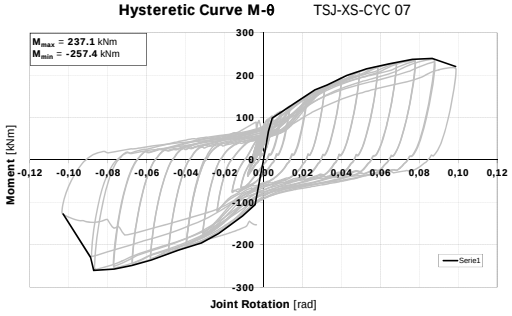

TSJ-XS-CYC 07

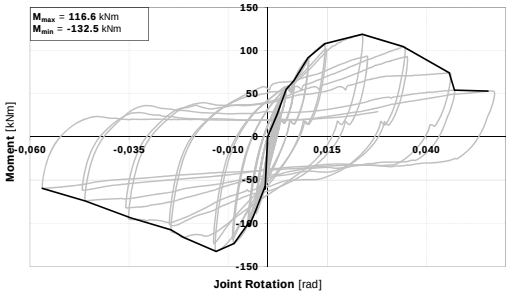

TSJ-M1 CYC08

(Fig. 17) contd….

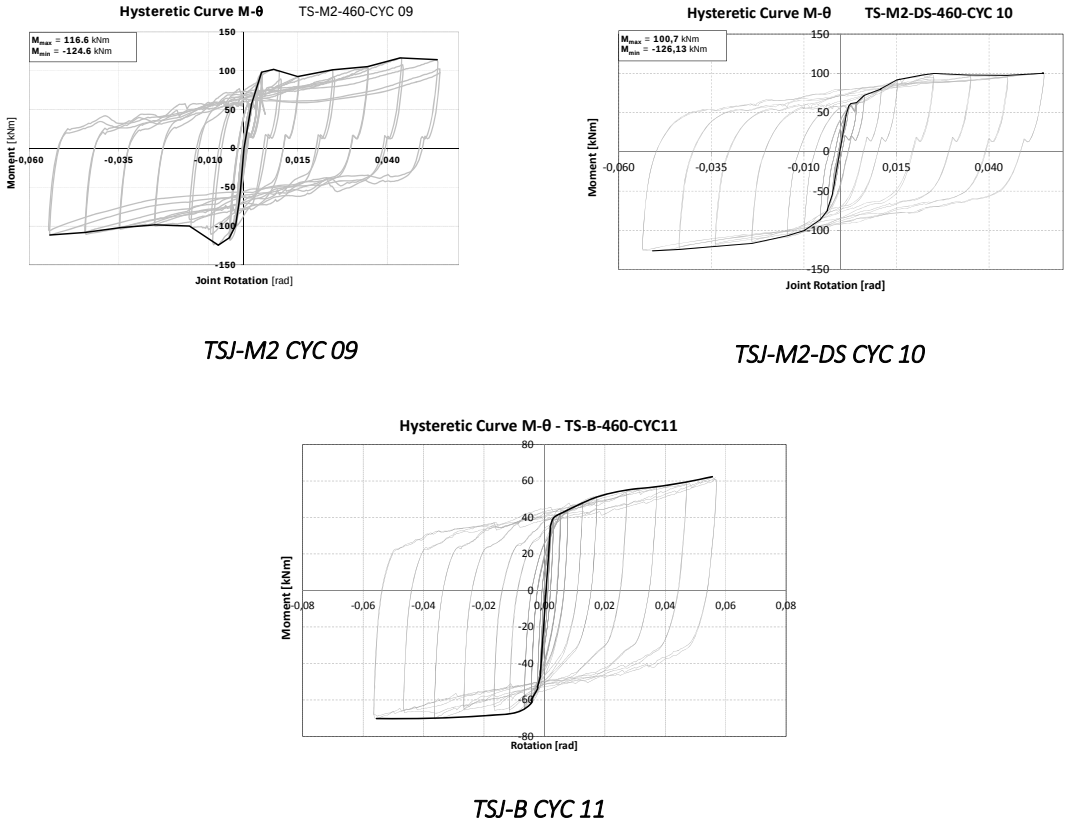

Fig. (17). Cyclic behaviour of the experimental tests.

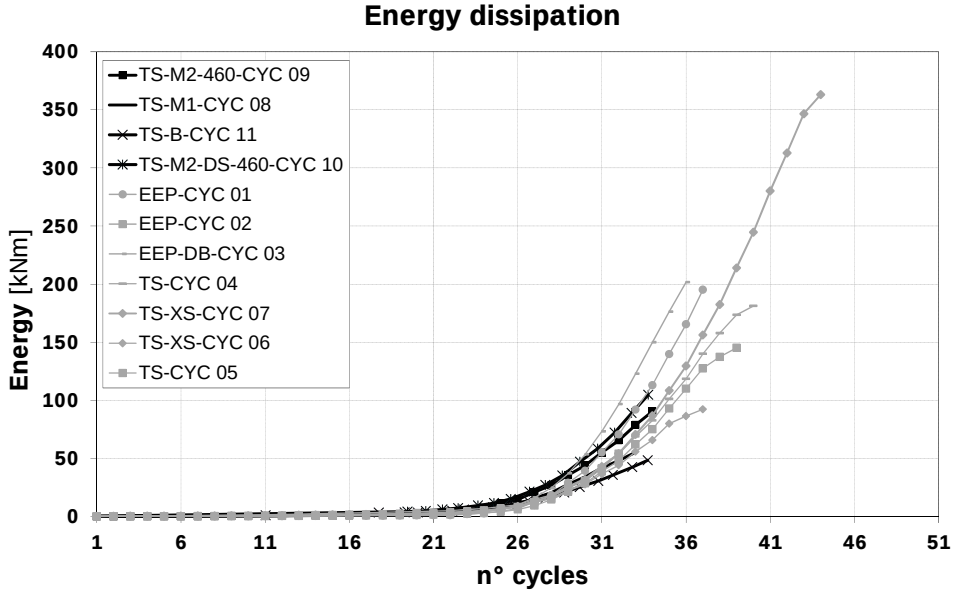

Fig. (18). Comparison in terms of energy Dissipation.

of energy dissipation occurs with respect to specimen EEP-DB CYC 03 was observed. Conversely, due to pinching phenomena, joints engaging in plastic range bolted components exhibited a significant reduction of energy dissipation, but the results show that, if properly detailed, they can develop a significant rotational capacity. In particular, even though the classical extended end-plate joints exhibited a quite poor energy dissipation capacity (EEP-CYC 02), the classical and X-shaped T-stub joints provided a high ductility supply. In fact, from (Fig. **18**) is worth to note that the joint which exhibited the highest ductility supply is TSJ-XS-CYC 07 which reached a rotational capacity equal to the 10%.

CONCLUSION

In the present paper, the results of a wide experimental research program on the cyclic response of beam-to-column jointsare discussed focusing the attention on the possibility of using the component approach as a design tool to govern, within the design process, the location of dissipative elements by properly imposing the weakest component. Under this point of view, it was underlined that all the experimental results confirmed the design choices.

In addition, the behaviors of traditional beam to column joints, such as extended end plate joints and double split tee joints, are compared with those of innovative joints. Aiming to adopt a structural solution easy to restore after a severe seismic event, two typologies of innovative joints have been considered: double split friction tee stub beam-to-column joints and X-shaped tee stub beam-to-column joints. In particular, the response in terms of energy dissipation and the shape of the hysteresis loops of the proposed innovativebeam-to-column joints have been compared with those of a traditional joints. The results obtained are very encouraging, confirming the merit of both innovative proposed joint solutions. In particular, the experimental tests have confirmed that the strategy of adopting friction pads between the components of bolted connections can be effective for the ambitious goal of damage prevention while a significant enhancement of the energy dissipation capacity and of the cyclic behavior can be obtainedfastening the beam to the column by means of dissipative X-shaped T-stubs.

CONFLICT OF INTEREST

The authors confirm that this article content has no conflict of interest.

ACKNOWLEDGEMENTS

Declared none.

REFERENCES

[1] F. Mazzolani, and V. Piluso, "Theory and Design of Seismic Resistant Steel Frames", London: E & FN Spon, an Imprint of Chapman & Hall, 1996.

[2] V. Piluso, and G. Rizzano, "Experimental Analysis and modelling of bolted T-stubs under cyclic loads", *Journal of Constructional Steel Research*, vol. 64, pp. 655-69, 2008.

[3] M Latour, and G Rizzano, "Full strength design of column base connections accounting for random material variability", *Engineering Structures*, vol. 48, pp. 458-471, 2013c.

[4] C. Faella, R. Montuori , V. Piluso, and G. Rizzano, "Failure mode control: economy of semi-rigid frames", In: *Proceedings of the XI European Conference on Earthquake Engineering*, Paris, 1998.

[5] CEN, Eurocode 3: *Design of steel structures - Part 1-1*: General rules and rules for buildings., 2005a.

[6] CEN, Eurocode 3: *Design of steel structures - Part 1-8*: Design of joints., 2005b.

[7] CEN, Eurocode 8: *Design of structures for earthquake resistance - Part 1*: General rules, seismic actions and rules for buildings., 2005c.

[8] C. Bernuzzi, R. Zandonini, and P. Zanon, "Experimental analysis and modelling of semi-rigid steel joints under cyclic reversal loading", *Journal of Constructional Steel Research*, vol. 2, pp. 95-123, 1996.

[9] I. Clemente, S. Noè, and G.A. Rassati, "Experimental and Numerical analysis of the cyclic behaviour of t-stub components", In: *Proceedings of XX CTA Conference*, Ischia, 2005.

[10] A.G. Coelho, *Characterization of the ductility of bolted end plate beam-to-column steel connections*. Coimbra: Universidade de Coimbra, 2004.

[11] C. Faella, V. Piluso, and G. Rizzano, *Structural steel semi-rigid connections*. Boca Raton: CRC Press, 2000.

[12] J. Jaspart, F. Wald, K. Weynand, and N. Gresnigt, "Steel column base classification," *HERON*, vol. 53, 2008.

[13] J.P. Jaspart, "*Etude de la semi-rigidite des noeuds Poutre-Colonne et son influence sur la resistance et la stabilite des ossature en acier*", PhD Tesis ed. Liege: University of Liege, Belgium, 1991.

[14] C. Faella, V. Piluso, and G. Rizzano, "A new method to design extended end plate connections and semirigid braced frames", *Journal of Constructional Steel Research*, vol. 41, pp. 61-91, 1997.

[15] AISC, *Seismic Provisions for Structural Steel Buildings*. Chicago, Illinois, 2005.

[16] F. Iannone, M. Latour, V. Piluso, and G. Rizzano, "Experimental analysis of bolted steel beam-to-column connections: Component identification", *Journal of Earthquake Engineering*, vol. 15, no. 2, pp. 214-44, 2011.

[17] M. Latour, and G. Rizzano, "A theoretical model for predicting the rotational capacity of steel base plate joints", *Journal of Constructional Steel Research*, pp. 88-99, 2013a.

[18] M. Latour, and G. Rizzano, "Innovative connections for timber panel buildings", *International Journal of Earthquake Engineering*, 2014c.

[19] M. Latour, V. Piluso, and G. Rizzano , "Experimental analysis and mechanical modelling of t-stubs with four bolts per row", *Journal of Constructional Steel Research*, pp. 158-174, 2014a.

[20] M. Latour, V. Piluso, and G. Rizzano, "Experimental analysis of friction materials for supplemental damping devices", *Construction and Building Materials*, 2014b.

[21] M. Latour, V. Piluso, and G. Rizzano, "Rotational behaviour of comun base plate connections: experimental analysis and modelling", *Engineering Structures*, pp. 14-23, 2014.

[22] D. Dubina, N. Montreau, A. Stratau, D. Grecea, and R. Zaharia, "Testing program to evaluate behavior of dual steel connections under monotonic and cycli loading", In: *Proceedings of the 5th European Conference on Steel and Composite Structures*, Graz, Austria, 2008.

[23] A.Y. Elghazouli, "Seismic design of steel frames with partial strength connections", In: *Proceedings of the 6th SECED Conference on Seismic Design Practice*, Oxford, UK, 1998.

[24] M. Latour, V. Piluso, and G. Rizzano, "Experimental analysis of innovative dissipative bolted double split tee beam-to-column connections", *Steel Construction*, vol. 4, pp. 53-64, 2011.

[25] A. Longo, R. Montuori, and V. Piluso, "Failure mode control of X-braced frames under seismic actions", *Journal of Earthquake Engineering*, pp. 728-59, 2008.

[26] A. Longo, R. Montuori, and V. Piluso, "Theory of plastic mechanism control for mrf-cbf dual system and its validation", *Bullettin of Earthquake Engineering*, 2014.

[27] A. Longo, R. Montuori, and V. Piluso, "Theory of plastic mechanism control of dissipative truss moment frames", *Engineering Structures*, vol. 37, pp. 63-75, 2012.

[28] A. Longo, R. Montuori, and V. Piluso, "Failure mode control and seismic response of dissipative truss moment frames", *Journal of Structural Engineerin*g, vol. 138, pp. 1388-97, 2012.

[29] R. Montuori, E. Nastri, and V. Piluso, "Advances in theory of plastic mechanism control: closed form solution for mr-frames", *Earthquake Engineering and Structural Dynamics*, 2015.

[30] K.D. Kim, and M.D. Engelhardt, "Monotonic and cyclic loading models for panel zones in steel moment frames", *Journal of Cosntructional Steel Research*, vol. 58, pp. 605-635, 2002.

[31] K.S. Moore, J.O. Malley, and M.D. Engelhardt, *Design of Reduced Beam Section (RBS) Moment Frame Connections*. Moraga: AISC Structural Steel Educational Council, 1999.

[32] M.D. Engelhardt, T. Winneberger, A.J. Zekany, and T.J. Potyraj, "Experimental investigation of dogbone moment connections", In: *Proceedings of National Steel Construction Conference*, Chicago, 1997.

[33] Joint Venture SAC, "*Iterim Guidelines Advisory No.1*", 1997.

[34] M. Latour, and G. Rizzano, "Experimental behavior and mechanical modeling of dissipative T-Stub connections", *Journal of Structural Engineering*, vol. 138, no. 2, pp. 170-182, 2012.

[35] M. Latour, and G. Rizzano, "Cyclic behaviour and modelling of dissipative connectors for cross-laminated timber panel buildings", *Journal of Earthquake Engineering*, 2015.

[36] M.A. Miner, "Cumulative Damage in Fatigue", *ASME Journal of Applied Mechanics*, vol. 67, pp. A159-A164, 1945.

[37] M. Latour and G. Rizzano, "Cyclic behavior of dissipative X-shaped double split tee joints", J*ournal of Constructional Steel Research*, 2015.

[38] M. Latour, V. Piluso, and G. Rizzano, "Experimental behaviour of friction T-stub beam-to-column joints under cyclic loads", *Steel Construction*, 2013.

[39] M. Latour, V. Piluso, and G. Rizzano , "Cyclic modeling of bolted beam-to-column connections: component approach", *Journal of Earthquake Engineering*, vol. 15, no. 4, pp. 537-63, 2011.

[40] R. Montuori, E. Nastri, and V. Piluso, "Theory of plastic mechanism control for the seismic design of braced frames equipped with friction dampers", *Mechanics Research Communications*, vol. 58, pp. 112-123, 2014.

[41] R. Montuori, V. Piluso, and M. Troisi, "Innovative structural details in MR-frames for free from damage structures", *Mechanics Research Communications*, vol. 138, pp. 146-56, 2014.

[42] I.D. Aiken, P.W. Clark, and J.M. Kelly, "Design and Ultimate-Level Earthquake Tests of a 1/2.5 Scale Base-Isolated Reinforced-Concrete Building", In: *Proceedings of ATC-17-1 Seminar on Seismic Isolation, Passive Energy Dissipation and Active Control*, San Francisco.California, 1993.

[43] C. Christopoulos, and A. Filiatrault, *Principles of passive supplemental damping and seismic isolation*. Pavia: IUSS PRESS, 2006.

[44] T.T. Soong, and B.F. Spencer Jr, "Supplemental energy dissipation: State-of-the-art and state-of-the-practice", *Engineering Structures*, vol. 24, pp. 243-59, 2002.

[45] C. Heistermann, *Behaviour of Pretensioned Bolts in Friction Connections*. Lulea: Lulea University of Technology, 2011.

[46] Schnorr, *Handbook for Disc Springs*, Eberhard Fromm and Wolfgang Kleiner, Ed. Heilbronn: Adolf Schnorr GmbH, 2003.

Received: August 25, 2014 Revised: September 30, 2014 Accepted: November 11, 2014